Intercellular Communication in Normal and Regenerating Rat Liver: A Quantitative Analysis

DAVID J. MEYER, S. BARBARA YANCEY, and JEAN-PAUL REVEL, *with an appendix by* ARTHUR PESKOFF

Divison of Biology, California Institute of Technology, Pasadena, California 91125 and the Departments of Physiology and Biomathematics, University of California, Los Angeles, California 90024

ABSTRACT We have compared intercellular communication in the regenerating and normal livers of weanling rats. The electrophysiological studies were conducted at the edge of the liver, and we have found that here as elsewhere in the liver there is a dramatic decrease in the number and size of gap junctions during regeneration. The area of hepatocyte membrane occupied by gap junctions is reduced 100-fold 29–35 h after hepatectomy. By combining observations made with the scanning electron microscope with our freeze fracture data we have estimated the number of "communicating interfaces" (areas of contact between hepatocytes that include at least one gap junction) formed by hepatocytes in normal and regenerating liver. In normal liver a hepatocyte forms gap junctions with every hepatocyte it contacts (~6). In regenerating liver a hepatocyte forms detectable gap junctions with, on average, only one other hepatocyte.

Intercellular spread of fluorescent dye and electric current is reduced in regenerating as compared with normal liver. The incidence of electrical coupling is reduced from 100% of hepatocyte pairs tested in control liver to 92% in regenerating liver. Analysis of the spatial dependence of electrotonic potentials indicates a substantial increase in intercellular resistance in regenerating liver. A quantitative comparison of our morphological and physiological data is complicated by tortuous pattern of current flow and by inhomogeneities in the liver during regeneration. Nevertheless we believe that our results are consistent with the hypothesis that gap junctions are aggregates of channels between cell interiors.

Cells in most vertebrate tissues, in embryos, in tissue culture, and in many invertebrates are interconnected by low-resistance pathways permeable to ions and small molecules. Generally speaking, this pathway behaves as a simple aqueous tunnel between cell interiors (see references 5 and 33 for recent reviews). There is strong, but as yet only circumstantial evidence that the gap junction is the site of this intercellular pathway.

Early evidence for the role of specialized cell junctions in electrical coupling between excitable cells came from the work of Barr et al (2, 3, 12) and Dreifuss et al (13). Potter et al (46) as well as Loewenstein and Kanno (34) obtained evidence for such junctions in nonexcitable tissues. Studies of the electrotonic synapses of the crayfish medial giant axon showed that increases in the junctional resistance between axon segments were associated with the disappearance of gap junctions between axonal membranes (41). Subsequently, two studies specifically associated the presence of gap junctions with intercellular communication. In the brown fat of newborn mice and in baby hamster kidney (BHK) cells grown in tissue culture, systems in which electrotonic coupling had already been demonstrated (20, 52), Revel et al (49) showed that gap junctions were the only form of specialized cell contact present. Gilula et al (24) demonstrated electrical coupling of cells and intercellular transfer of radioactively labeled nucleotides in cultures of hamster fibroblast cell lines that formed gap junctions but not in cultures of variant cell lines in which gap junctions were not observed.

Structural studies of gap junctions have provided further evidence for their role in intercellular communication (26).

THE JOURNAL OF CELL BIOLOGY · VOLUME 91 NOVEMBER 1981 505-523

Low-angle x-ray diffraction (37) and analysis of negatively stained junctions by low-dose electron microscopy (55) indicate the presence of a pore within the subunits or connexons that comprise the gap junction. Thus the array of membrane particles that comprises the gap junction may represent aggregates of intercellular channels. The finding that the resistance of the intercellular pathway varies approximately inversely with the size of gap junctions in reaggregated Novikoff hepatoma cells (30) is consistent with this hypothesis.

Although there is little opposition to the idea that gap junctions mediate intercellular communication, it is not clear whether they are the only structures that do so. For example, after EGTA-dispersed Novikoff hepatoma cells are allowed to reaggregate, electrical coupling is observed before mature gap junctions can be demonstrated (53). In some vertebrate longitudinal smooth muscle in which cells are presumed to be electrically coupled, gap junctions have not been observed or have been observed only rarely (11, 19, 22, 23). In addition, tight junction-like elements, rather than gap junctions, are found in "partially communication competent" cells (32). Though all these results could be explained by the presence of occasional connexon pairs that would be difficult to identify, it is clear that the question of whether gap junctions are necessary for cell-cell communication is not yet resolved.

We present here a detailed physiological and morphological study of the regenerating liver of weanling rats that further tests the hypothesis that gap junctions mediate intercellular communication. Between 28 and 36 h after partial hepatectomy, there is a rapid fall in the number and size of gap junctions between hepatocytes in the remaining lobes (60, 62). Morphometric analysis reveals that there is a drastic reduction in the area of gap junctions in regenerating as compared with normal liver (60). According to present understanding, the conductance of the intercellular pathway for current flow and the intercellular spread of tracer molecules should be reduced at times when gap junctions are small and few in number. Our results support the hypothesis although the extent of electrical coupling found was greater than that expected on the basis of the morphological data. Preliminary reports of some of these data have been presented (38, 48).

MATERIALS AND METHODS

Animals

Three- to four-week-old Sprague-Dawley rats were partially hepatectomized as previously described (60, 62). Animals were killed at various times between 28 and 36 h after the surgery. Control rats were obtained from the same litters and were also studied at 3–4 wk of age.

Electrophysiology

Rats were anesthesized with ether and the caudal portion of the right lateral lobe of the liver was rapidly dissected from the animal and placed in warmed, oxygenated physiological saline (25). A thin segment (1 × 5 mm) of the free edge of the lobe was cut away and mounted in a lucite perfusion chamber on the stage of a modified compound microscope. The liver sample was perfused with a constant flow (2 ml/min) of oxygenated physiological saline warmed to 37°C. The temperature of the perfusate was monitored constantly during the course of an experiment with a miniature thermistor probe (Yellow Springs Instrument Co., Yellow Springs, Ohio). Microelectrodes were drawn from 1.2 mm outer diameter (O.D.) omega dot borosilicate tubing (Fredrick Haer, Brunswick, Maine) using a horizontal type puller (Industrial Science Associates, Woodside, N.Y.). With 3 M KCl as the electrolyte, electrode resistance was typically 20–30 mΩ in saline. Electrode tips were bent to an angle of ~45° (28) to permit the use of objectives with large numerical apertures and short working distances.

Current and voltage microelectrodes were connected to high input impedance amplifiers (W-P Instruments, Inc., New Haven, Conn., model M701). Stimulus pulses were produced by an Anapulse stimulator and associated photon coupled stimulus isolators (W-P Instruments, Inc. model 302-T). Voltage pulses were converted to constant current pulses by the M701 amplifiers. The stimulus currents were monitored with a virtual ground circuit. Electrophysiological data were measured either directly from an oscilloscope display (Tektronix 5111, Tektronix, Inc., Beaverton, Ore.) or from penwriter records.

Electrical coupling between hepatocytes was studied by inserting two microelectrodes into cells within 50–100 μm (2–5 cell diameters) of the edge of the liver; one of the electrodes was used for passing current while the other was used for measuring the resulting electrotonic potential. The distance between the microelectrode tips was measured with an eyepiece micrometer.

For dye-spread studies, electrodes were filled with 0.4 M 6-carboxyfluorescein (Eastman Kodak) prepared according to the method of Brink and Dewey (7). Alternatively, a 5% solution of Lucifer Yellow CH (a gift of W. W. Stewart, National Institutes of Health, Bethesda, Md.) was dissolved in 1 M LiCl (56). Cells were filled with either dye by iontophoresis: 10^{-8} ampere negative current pulses, 35 ms in duration, repeated every 60 ms. For dye-injection experiments, one hepatocyte was penetrated with a dye-filled electrode while a nearby cell (~50 μm distant) was penetrated with a KCl electrode. For some experiments, two dye-filled electrodes were used. Iontophoresis of dye resulted in electrotonic potentials that were detected with the second electrode. Monitoring the electrotonic potential during iontophoresis was useful for detecting deteriorating impalements. We rejected cells in which a decrease of 2 mV or greater in the electrotonic potential or in resting potential was detected over the course of the injection.

Light Microscopy

We used a Zeiss WL microscope equipped for epifluorescence for these experiments. The microscope was modified so that focusing was accomplished by moving the microscope body while the stage remained stationary. The microscope objective was heated with a coil of nichrome wire to prevent condensation of water vapor from the perfusing solution. Fluorescence was excited by epiillumination with wavelengths below 485 nm.

Dye spread was studied both in living tissue and in fixed, sectioned liver. In the former instance, the tissue in the perfusion chamber was photographed at timed intervals with a camera attached to the microscope. The samples were sometimes simultaneously transilluminated with dim visible light. For examination of sectioned tissue, injected specimens were fixed in 4% formaldehyde, dehydrated in ethanol, and embedded in diepoxyoctane and nonenylsuccinic anhydride (Aldrich Chemical Co., Milwaukee, Wis.) (36). Sections 0.5–1.0 μm in thickness were cut on a Reichert ultramicrotome. Photomicrographs were taken with a Zeiss C35mm camera using Tri X film rated at ASA 800 and developed in diafine. Exposures of bright-field photomicrographs were determined with a photometer whereas dark-field exposures were 10 s in duration. Processing conditions for film and prints were held constant to permit direct comparison of data from regenerating and control livers. Magnifications were determined from photographs of a stage micrometer.

Electron Microscopy

The procedure for fixation and freeze fracture was identical to that described by Yancey et al. (60) except that we studied samples taken from the liver's edge. For scanning electron microscopy (SEM), livers were fixed by perfusion through the portal vein with 2.5% glutaraldehyde in Earle's balanced salt solution or in cacodylate buffer. Measurements made on liver samples perfused at physiological pressures or at higher pressures gave similar results. Fixation was continued for an additional 4 h by immersing the right lateral lobe in the same solution. A portion of the free edge was dissected away, postfixed in osmium tetroxide, and partially dehydrated in ethanol (up to 90% ethanol). At this point, some of the samples were broken normal to the intact free edge. Dehydration was then completed and followed by critical point drying from liquid CO_2. Other pieces were broken after drying. Pieces of tissue with a recognizable free edge were mounted on aluminum stubs and coated with a thin layer of gold-palladium alloy. Specimens were examined with an ETEC autoscan scanning electron microscope at 10 or 20 kV.

Morphometric analysis

To assess quantitative changes in gap junctions, we examined freeze-fracture faces of hepatocyte cell membranes near the edge of the right lateral lobe of the liver in a Philips 301 electron microscope (60). The replicas were mounted on 50-mesh grids, and hepatocyte faces were examined in their entirety at × 13,000. The micrographs were printed at a final magnification of × 30,000. The area of gap junctions and hepatocyte membrane were determined by digitizing the outlines of the regions of interest (with an electronic digitizing tablet) and computing the corresponding areas (16). The relevant membrane is the smooth portion of hepatocyte membrane extending from the bile canaliculus toward the

periphery where the cell surface is thrown into numerous irregular projections as it nears the sinusoids and space of Disse (see Fig. 1). The true extent of the contact area between hepatocytes was estimated from measurements made on broken liver samples (see above) viewed by SEM. Hepatocytes were photographed with their contact surfaces oriented approximately normal to the electron beam. The length and width (distance from the lateral border of the bile canaliculus to the medial edge of the microvilli that border the space of Disse) of the contact area were measured on photomicrographs with the digitizing tablet. The distance from the bile canaliculus to the microvilli was similarly measured on suitable freeze-fracture interfaces. The ratio of the average width measured in freeze-fracture specimens to that measured in SEM specimens was used as a correction factor to compensate for differences in specimen preparation. The appropriate correction factor (width in freeze-fracture replica/width in SEM specimen) was found to be 1.2 in both normal and regenerating liver. This has allowed us to calculate the average area of a contact face as well as the average true area of junctions per hepatocyte-to-hepatocyte interface. Calculation of the specific membrane resistance of hepatocytes required determination of the density of the surface membrane of hepatocytes in rat liver. The required densities were calculated using a modification of the method of Weibel et al (57). Thin sections were cut from the area of normal and regenerating rat liver that was used for electrical measurements. The sections, after staining with uranyl acetate and lead citrate, were examined in a Philips 301 electron microscope at 80 kV and photographed. Micrographs were printed at a final magnification of × 9,200. The cell perimeter (length of hepatocyte plasma membrane) and the area of sections (excluding grid bars) were estimated by digitizing the outlines of structures and using appropriate computational methods. The ratio of the length of hepatocyte plasma membrane to the area of tissue examined was used as an estimate of hepatocyte plasma membrane density.

RESULTS

Liver Structure and Analysis of the Cell Junctions in Normal and Regenerating Liver

MORPHOLOGY OF THE LIVER: We have investigated the structure of the thin free border of regenerating and control liver with scanning electron microscopy to gain an understanding of the potential pathways of intercellular communication in the regions used for our physiological studies. The architecture at the free edge of the liver closely resembles that observed by others in previous studies of liver structure (15, 39, 40, 56). In SEM the hepatocytes typically are seen in single rows that represent fractures through the liver cords or laminae (Figs. 1 and 2); laminae anastomose extensively with one another to form a complex three-dimensional network. As a row of hepatocytes lies between two sinusoids (Figs. 1 and 2), most hepatocytes have at least two free surfaces that border a space of Disse. The remaining cell membrane is closely apposed to some six other hepatocytes except for the small portion of cell surface that is part of the wall of the bile canaliculus (Fig. 1). The apposed cell surfaces, smooth in the pericanalicular area, are thrown into folds and microvilli in the juxtasinusoidal region. As shown by the study of replicas of freeze-fractured liver and of thin sections, gap junctions are found only in the smooth region. Both tight and gap junctions can occasionally be detected in SEM samples. When the two halves of a gap junction remain adherent, a scar is formed on the cell from which the junction half is pulled, and extra, scablike material is left on the other (1).

In regenerating liver the free edge is thickened by the addition of more parenchymal tissue. SEM of tissue taken from the edge of regenerating liver shows that in some cases the laminae are more than a single cell in width, and one can occasionally find cells that are apparently in mitosis. Intercellular relationships are otherwise unaltered at this level of detail (Fig. 3). Structures assumed to represent gap junctions are not found.

Previous studies in this laboratory (60, 62) have established the time-course of the disappearance and reappearance of gap junctions between hepatocytes using randomly selected samples of tissue from the right lateral lobe of the regenerating liver. We have repeated some of these measurements in normal and regenerating liver to document the process of gap junction disappearance in the specific regions studied electrophysiologically. Four of the seven regenerating liver preparations examined by freeze-fracturing were also studied electrophysiologically before fixation to control for possible changes in the complement of gap junctions during the electrical measurements.

Examination of hepatocyte surface membranes in freeze-fractured samples revealed the presence of large gap junctions in control liver (Fig. 4). The density of gap junctions was such that one could find at least one for every 25 μm^2 of interface between two adjacent hepatocytes. Because the total area of contact between adjoining hepatocytes is ~100 μm^2 (as determined from scanning electron micrographs; see below) one can infer that several junctions are present on each interface. In those instances where gap junctions can be recognized in the SEM, several can in fact be found on each contact interface. Between 30 and 35 h after partial hepatectomy, gap junctions were rarely seen in freeze-fracture replicas of hepatocyte membrane. When gap junctions were encountered they generally numbered two or more per interface but were very small and usually close to the strands of the tight junction (Fig. 5). The total length of tight-junctional strands per unit length of the canalicular margin of hepatocytes was unchanged (unpublished results).

MORPHOMETRY OF GAP JUNCTIONS: The pictorial information obtained by SEM and by freeze cleaving was used to measure various parameters of the distribution of gap junctions on the hepatocyte surface in both control and regenerating liver. An interpretation of the morphometric data presented in Table I must take into account the fact that the freeze-fracture technique samples only a small part of the hepatocyte surface. On average, freeze-fracture interfaces measure ~40 μm^2. Thus we typically observed only a portion of the contact area between two hepatocytes that is available for formation of gap junctions. The actual extent of this contact area was estimated from measurements made on hepatocytes from broken edges of normal and regenerating liver viewed by SEM where the entire interface can be observed.

Using the techniques described in Materials and Methods, we calculated that the total contact area between two hepatocytes in specimens from regenerating liver prepared for freeze-fracture was ~ 100 μm^2. Because examination of stereo pairs of scanning electron micrographs suggests that each hepatocyte contacts on average six other hepatocytes, the total contact area is ~600 μm^2. Hence, if there were only one gap junction on the surface of each hepatocyte in regenerating liver there would be only a 40/600 or 7% chance that it would be observed on a freeze-fracture interface. This line of argument can be generalized to estimate the distribution of gap junctions in the regenerating liver.

We define communicating interface as a membrane interface with at least one gap junction as observed in freeze-fracture replicas. A single communicating interface is therefore theoretically the minimum needed for exchanges to take place between two neighbouring cells. There must be at least two communicating interfaces per cell to form a linear string of communicating hepatocytes, and some cells must have three to form a branching network. In normal liver the number of communicating interfaces (R) per cell was estimated to be between 12 and 14, but in regenerating liver it is only between 0.5 and 1.5, on the average (Table I). If the hepatocyte population is assumed to be heterogeneous with respect to the distribution of

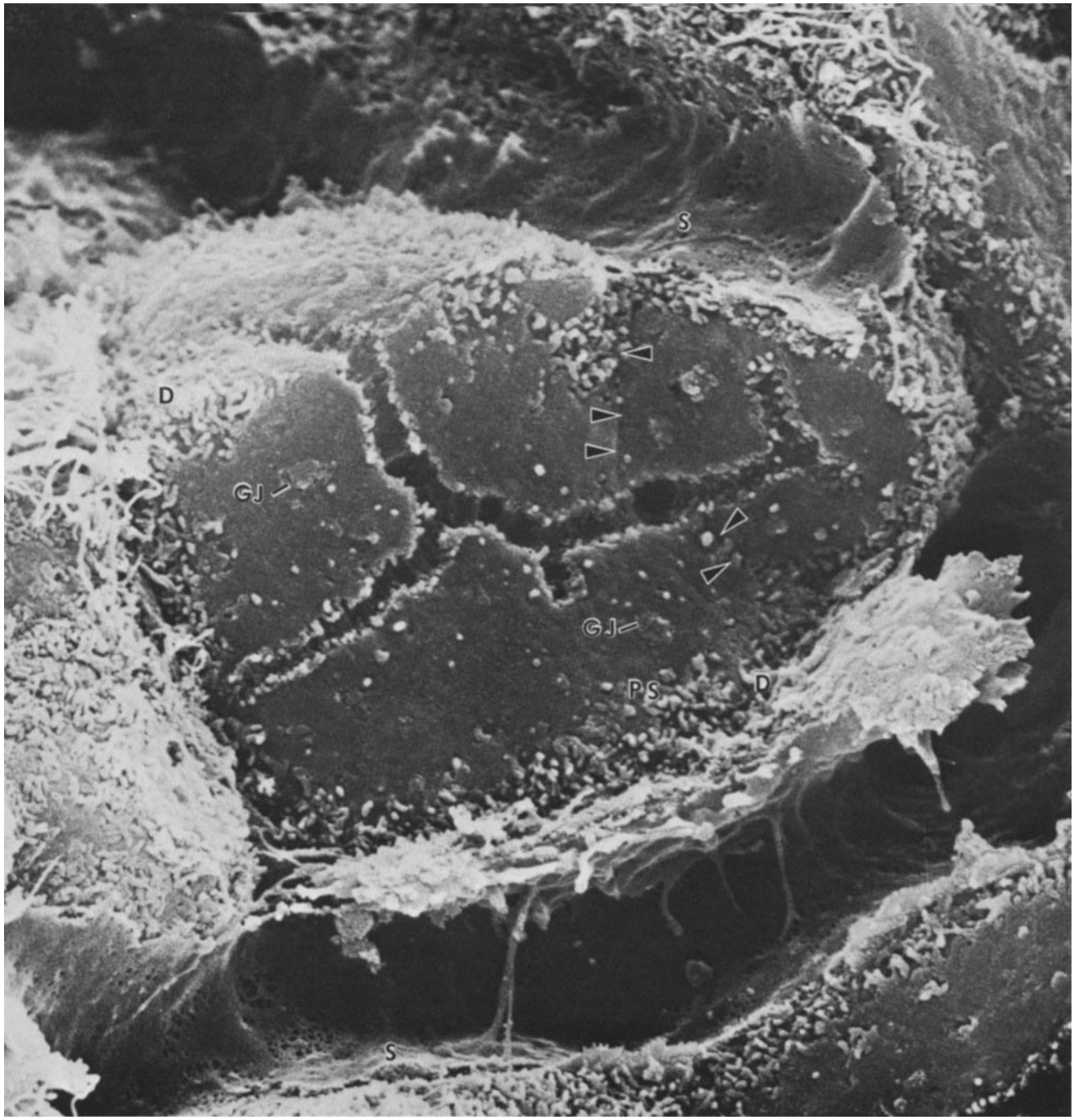

FIGURE 1 A piece of normal perfused liver viewed in the scanning electron microscope demonstrates the relationship of liver cells to each other and features of hepatocyte surface structure. The bile canaliculus is seen as a meandering open channel with occasional short side branches on what used to be the contact interface between now separated adjacent cells. The contact interface itself appears rather smooth. It is bounded on two sides by the perisinusoidal (*PS*) area which is studded with stubby microvilli similar to those found in the space of Disse (*D*), and on the other two by cell boundaries where three hepatocytes used to contact, often similar in appearance to the perisinusoidal area (arrows). Scars and scabs probably represent regions that had been occupied by large gap junctions (*GJ*). The two halves of these structures remain attached to each other when the cells were pulled apart during specimen preparation. Coursing between the hepatocytes are the sinusoids (*S*) lined by a thin endothelium perforated by patches of fenestrae. The sinusoids are roughly circular in cross section and form a three-dimensional lacework interdigitating with a similar lacework of hepatocytes. The density of these two networks and the relative sizes of the structural components give the impression, in sections, of alternating wall and channels, when in fact the real structure is much more complex.

communicating interfaces then the range of R will be greater.

The number of communicating interfaces is not necessarily the same as the number of other hepatocytes with which any one hepatocyte forms gap junctions. This is because the size of an interface observed in freeze fracture is less than half the contact area between two hepatocytes. Hence our data cannot tell us whether, for example, an average of two communicating interfaces per hepatocyte means that both interfaces occur between two hepatocytes or that, on average, every hepatocyte forms gap junctions with two other hepatocytes. In regenerating

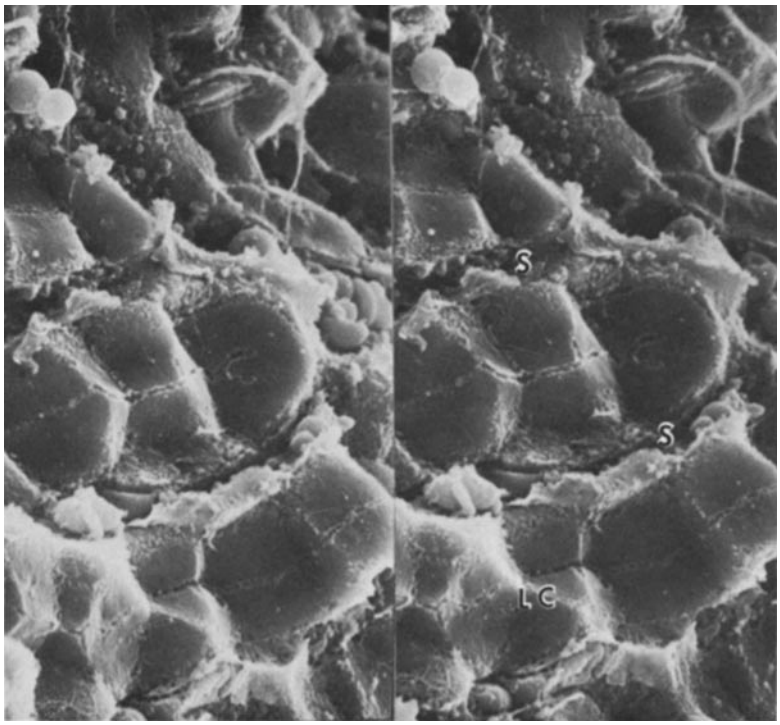

FIGURE 2 Viewed in stereo these micrographs intimate the complexity of the architecture of the liver. In monocular views, one is struck by the presence of cords of liver cells (*LC*) separated by sinusoids (*S*). The stereo view emphasizes the existence of two intertwined three-dimensional meshworks, one of which is formed by the sinusoids, the other by the hepatocytes. The prismatic shape of the hepatocytes is clearly seen and anastomoses between neighboring cords of liver cells are apparent. The sinusoids are channels, roughly circular in outline, that also branch and anastomose. The density of the meshworks formed respectively by the cellular and vascular elements, and the relative sizes of the components is such that, in two dimensions as in a single section, or on a fracture surface seen monocularly, one has the impression of alternating walls and channels. × 2,000.

liver, because R is small, the latter interpretation is reasonable, but this is certainly not true in the case of the controls.

STEREOLOGICAL DENSITY OF HEPATOCYTE PLASMA MEMBRANE: The density of hepatocyte plasma membrane in cells located at the edge of the caudal portion of the right lateral lobe (surface area/unit volume) was estimated as described in Materials and Methods. A total of 7,374 μm^2 of contiguous sections through normal liver containing 45 hepatocytes and 11,246 μm^2 of contiguous sections through regenerating liver including 87 hepatocytes was examined. The surface membrane density was found to be 0.355 m^2/cm^3 in control and 0.5015 m^2/cm^3 in regenerating liver. The surface membrane density for normal liver was found to be higher than the value (0.2840 m^2/cm^3) reported by Weibel et al. (57) who ignored the presence of microvilli on the hepatocyte surfaces bordering the bile canaliculi and sinusoids.

Physiology of Intercellular Communication in Normal and Regenerating Liver

Resting Potential of Normal and Regenerating Hepatocytes

The resting potential of normal hepatocytes ranged from −23 to −40 mV with an average near −31 mV. Results from six preparations are summarized in Table II. This is in substantial agreement with previous results from in vitro studies of normal rat liver (9, 18). In regenerating rat liver the resting potentials were larger, typically ranging between −35 and −55 mV. The average value was near −43 mV. A similar result has recently been reported by Wondergem and Harder (59). The results obtained in 15 experiments are shown in Table II. The origin of the difference in the resting potentials of normal and regenerating hepatocytes has not been investigated.

Transfer of Dye between Hepatocytes

We injected cells with 6-carboxyfluorescein to study the intercellular transfer of small molecules in normal and regenerating liver in the living state. The spread of dye was followed visually and photographed at timed intervals. We found that in electrically coupled cell pairs a considerable amount of dye spreads to neighboring cells even after times as short as 1 min (Fig. 6*a*). In three experiments the electrode containing dye was advanced through an impaled cell into a region where no resting potential was detected. Dye ejected iontophoretically under these circumstances rapidly outlined cells (Fig. 6*b*) rather than staining them intracellularly, suggesting that the dye spread easily by way of extracellular space.

To determine whether the impaled cells were hepatocytes, several cells were injected with the dye Lucifer Yellow, and injected cells were then studied after sectioning the tissue. In sections of both normal and regenerating liver the dye was always found within hepatocytes (Fig. 7).

The spread of 6-carboxyfluorescein was compared in normal and regenerating liver by taking photomicrographs at intervals of several minutes (Fig. 8). In each case the same parameters were used for dye injection and for photography; thus the results obtained in the two different conditions are directly comparable. Dye spread was always extensive in normal liver. In 19 of the 20 electrically coupled cell pairs tested in regenerating liver there was limited but clearly evident dye spread. In the remaining instance it was difficult to determine with certainty whether the glow that surrounded the cell injected with dye was due to the spread of dye or to the scattering of light from the injected cell. In cases of uncoupled or poorly coupled cell pairs in regenerating liver, at least one of the impaled hepatocytes did not allow a detectable amount of dye to spread to neighboring cells.

Spread of Electric Current in Normal and Regenerating Liver

We undertook an analysis of electric current flow in normal and regenerating liver to obtain a more quantitative picture of the changes in intercellular communication during regenera-

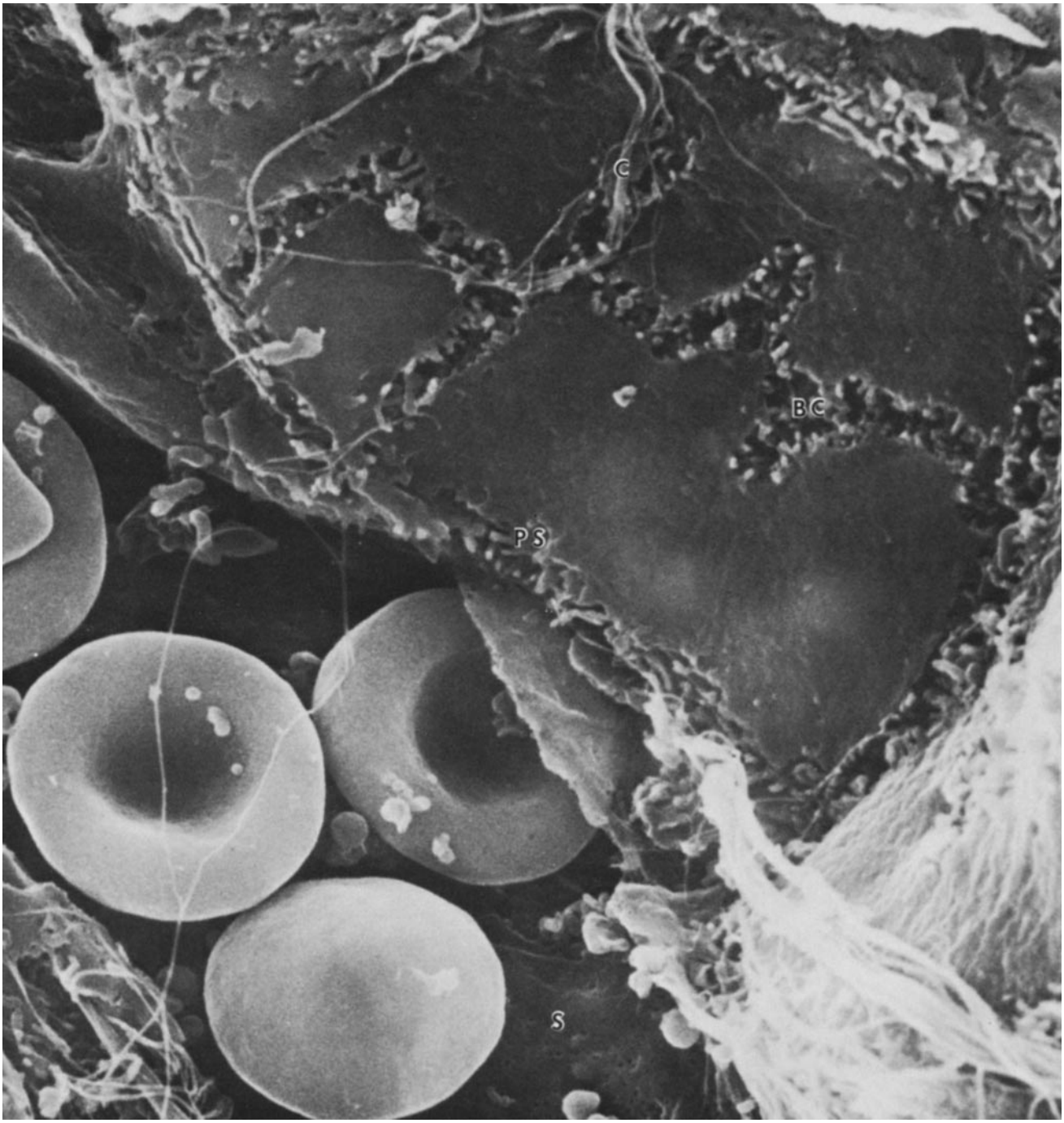

FIGURE 3 The intercellular contact faces of hepatocytes are shown here in regenerating liver ~30 h after partial hepatectomy, a time when junctional complement it at its minimum. The changes from the normal are rather subtle in preparations examined in the scanning electron microscope. This preparation shows that somewhat more elaborate branching pattern of the bile canaliculus (*BC*), which in regenerating liver often comes very close to the perisinusoidal region (*PS*). The contact interface itself lacks the scars and scabs that are often seen in normal liver, possibly a reflection of the small size and number of gap junctions. Some strands of collagen (*C*) artefactually overlie the surface of the hepatocytes.

tion. Because the hepatocytes form an electrically coupled network, electrophysiological techniques cannot directly provide information on particular cell interfaces even if the impaled cells are directly adjacent to one another. Studies of the spatial or time dependence of electrotonic potentials will reveal values of intercellular and membrane resistance only when the data are analyzed according to an appropriate model for the spread of current in a network of coupled cells.

CHARACTERISTICS OF ELECTROTONIC POTENTIALS: Electrotonic potentials were noticeably different in normal and regenerating liver (Fig. 9). The electrotonic potential when current and voltage microelectrodes were separated by 50 μm was consistently larger and had a slower time-course in regenerating than in control liver.

The steady-state amplitude of the electrotonic potential was proportional to the amplitude of the stimulus current pulse in both regenerating and control liver (Fig. 10). This result suggests a purely resistive pathway for current flow between cells

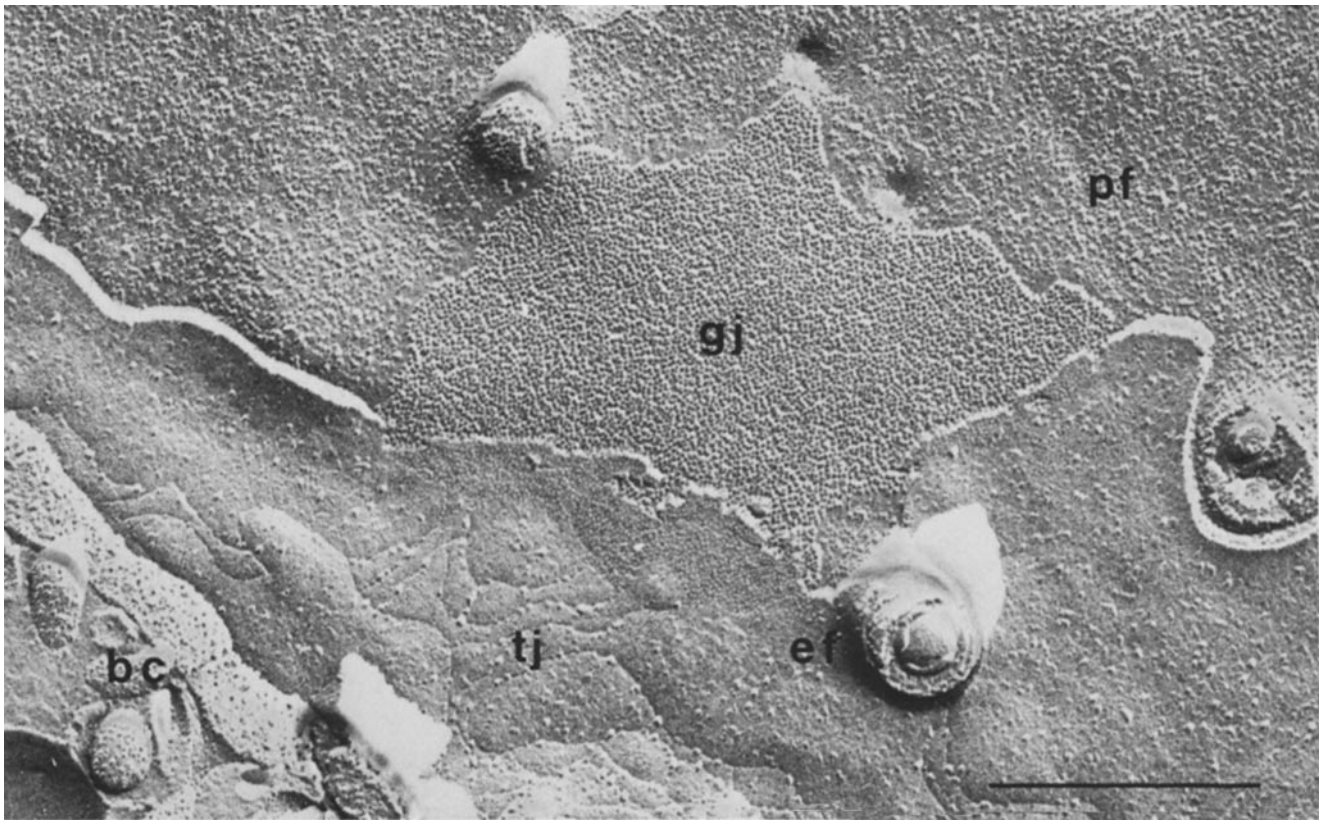

FIGURE 4 Freeze-fracture micrograph of a large gap junction (*gj*) at the interface between two hepatocytes in normal rat liver. The junction is composed of numerous particles forming an irregular lattice on the "P" face (*pf*) of the membrane of one hepatocyte and complementary pits in the "E" face (*ef*) of the membrane of the adjacent hepatocyte. Tight-junction grooves (*tj*) mark the perimeter of the bile canaliculus (*bc*). Bar, 0.5 μm. × 70,000.

in both preparations. The difference in the slopes of these plots for regenerating and control liver reflects differences in the resistance of the intercellular pathway for current flow in the two systems because for small interelectrode distances the magnitude of the electrotonic potential is virtually insensitive to any changes in membrane resistance (29).

The spatial dependence of the electrotonic potential was studied in six control and five regenerating liver preparations. Typical results are shown in Fig. 11. As has already been mentioned, for small (50 μm) interelectrode spacing, the electrotonic potentials in regenerating liver were considerably larger than those observed in control preparations. The magnitude of this potential fell more rapidly with distance in regenerating than in control preparations so that, when the interelectrode spacing was 150 to 200 μm, the electrotonic potentials in regenerating and in control preparations were similar in size; at 300 μm the potential in regenerating liver was usually smaller than in control liver. This result implies that the resistance of the junctional pathway for current flow is greater in regenerating than in control liver. The slower time-course of the electrotonic potential in regenerating as compared with control liver (Fig. 9) also results from an increase in the junctional and membrane resistance (see Eq. 16 of appendix; see also reference 29).

The magnitude of the electrotonic potential seen in regenerating liver at small electrode separations showed large variability (Fig. 11). We suspect that this was caused by variation in the electrical pathway between current and voltage electrodes. Such variation would arise if stimulus currents followed tortuous intercellular pathways in regenerating liver because some interfaces were devoid of junctional channels.

ANALYSIS OF THE SPATIAL DEPENDENCE OF ELECTROTONIC POTENTIALS: Estimation of the electrical resistance of the intercellular pathway requires a mathematical description of current flow in the liver. Such a theory must take into account the shape of the tissue, the fact that measurements were made within ~50 μm of the free border of the liver, and the presence of intercellular spaces. An accurate model must also consider the pathways taken by current as these are probably different in normal and regenerating liver (see Discussion). Although a complete description of current flow in the liver is not available, we have obtained estimates of the specific membrane resistance (Rm) and the specific intercellular resistance (Ri) by application of a model for current flow in a three-dimensional syncytium that has been solved for a wedge of tissue (Appendix). The model assumes that the tissue is isotropic and that there is an extensively interdigitated extracellular space with negligible resistance. The simplification of ignoring potential gradients within the extracellular space is justified for at least three reasons. First, microelectrodes in the extracellular space fail to detect a measurable electrotonic potential when a nearby hepatocyte is stimulated intracellularly. Second, the diffusion of 6-COOH fluorescein within the extracellular space (Fig. 6*b*) is extremely rapid when compared with intracellular dye spread. In fact the dilution of the dye due to its diffusion away from the injection site is so rapid that it is difficult to photograph. Judging from the fact that dye outlines individual hepatocytes, it appears that dye has free access to both the sinusoids and the narrow intercellular spaces where specialized cell contacts occur. Third, the structure of the liver suggests that the extracellular space should have negligible resistance. Each hepatocyte is bordered by

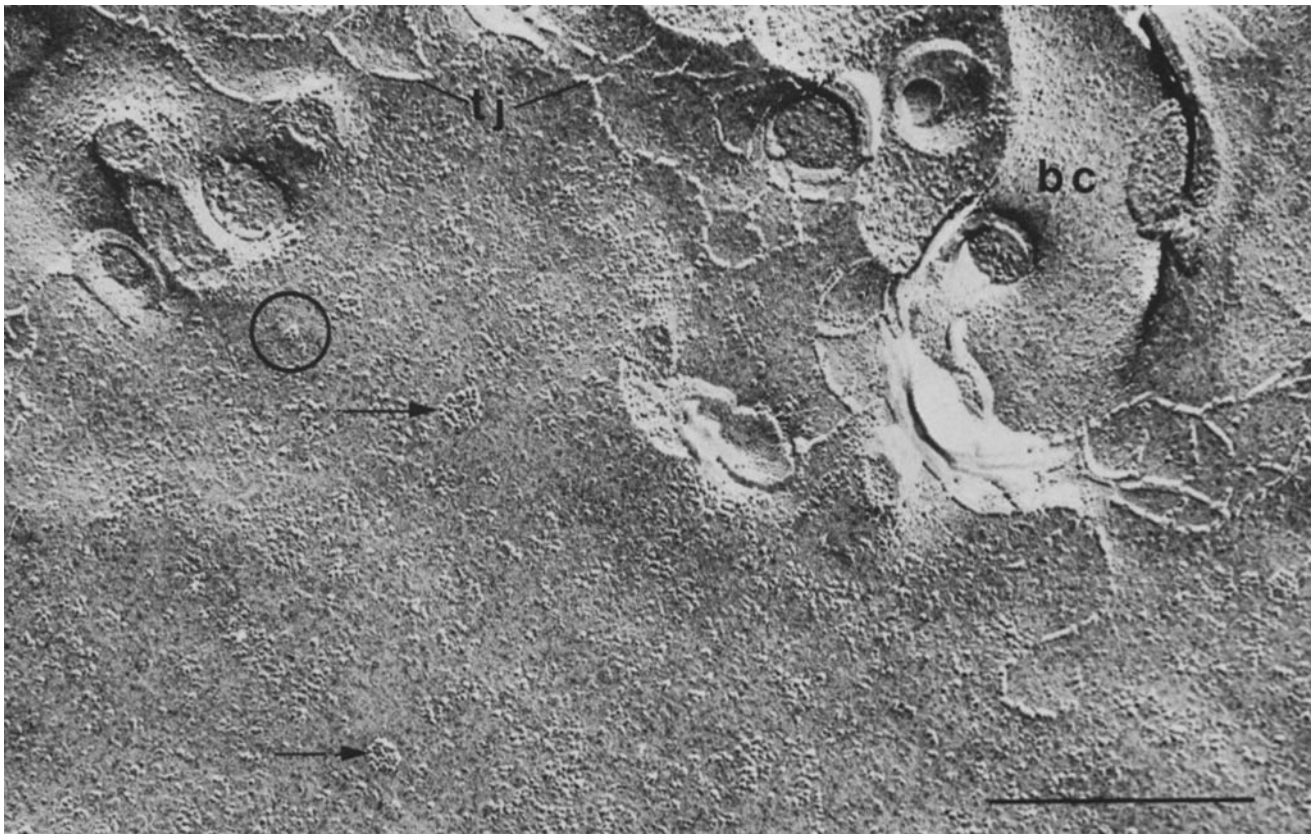

FIGURE 5 Freeze-fracture micrograph of the interface between hepatocytes in regenerating liver, 30 h after hepatectomy. Most interfaces sampled during the interval from 30–34 h after hepatectomy show no recognizable gap junctions. In this interface, small gap junctions (arrows) are present in a region of the membrane near the tight-junctional strands that parallel the bile canaliclus (*bc*). Some very small particle aggregates (circled) could represent physiologically competent junctional elements but were not included in our morphological estimates of junction number or area. Some aggregation or patchiness of nonjunctional intramembrane particles is apparent in this sample as it was in others obtained from specimens that were studied both morphologically and electrophysiologically. However, analysis of our morphological data compiled in Table I indicates that this presented no problem in the identification of gap junctions. Bar, 0.5 μm. × 70,000.

sinusoids on at least two surfaces (Fig. 2). Stereological measurements show that some 40% of the surface area of a hepatocyte borders the space of Disse (57). The sinusoids are broad channels, often >5 μm in cross section. The sinusoids are continuous with the venous system of the liver and therefore should be filled with a salt solution of low specific resistance. The values of Rm and Ri reported in Table III were those that yielded the best fit to the data points. The results of our computations indicate that Ri increases from ~3,000 Ω/cm in normal liver to ~30,000 Ω/cm in regenerating liver (Table III). Our results also indicate a small increase in Rm.

An alternative technique for measuring changes in the intercellular resistance is to measure changes in input resistance because the input resistance is expected to be proportional to Ri in a tissue made up of electrically coupled cells (29). We found that input resistance of rat liver was too low to measure with the single electrode technique. Use of two separate electrodes gave estimates of ~2×10^5 Ω. This is in reasonable agreement with the value that can be calculated from the results of Schanne and Coraboeuf (51) who used a double barrelled electrode to study hepatocytes in adult rat liver. Input resistance was ~1 order of magnitude larger in regenerating liver. These results should be regarded as tentative as it was difficult to obtain stable impalements of a hepatocyte with two electrodes and because there was considerable variability in the measured value of the input resistance measurements.

INCIDENCE OF COUPLING: Another way to assess the extent of coupling in the liver is to determine what fraction of the cell pairs studied are coupled. In normal liver, gap junctions occur between most if not all hepatocytes that contact one another. If gap junctions are the sites of the low-resistance pathway responsible for electrical coupling, then in normal liver all hepatocytes should be coupled. In contrast, in regenerating liver most areas of contact between hepatocytes are devoid of junctions, with the result that some fraction of the hepatocyte pairs studied should not be coupled.

For these experiments the spacing between current and voltage electrodes was between 50 and 100 μm. A pair of hepatocytes was considered to be coupled if a distinct electrotonic potential >1 mV was observed in response to a test pulse of 5×10^{-8} A.

A total of 354 pairs of hepatocytes were tested for coupling in seven control preparations. Coupling was observed in every case. Twelve regenerating liver preparations were also studied: of a total of 319 cell pairs studied in regenerating liver 24 were found not to be coupled (Table IV). The fraction of cell pairs that were not coupled was variable from sample to sample and bore no clear relation to the time within the 29- to 35-h "window" when hepatocytes in regenerating liver were studied. An analysis of the relationship between the occurrence of gap

TABLE I

Occurrence of Gap Junctions in Normal and Regenerating Liver

	Preparation number	Ratio of gap junctions to total membrane area	No. of interfaces sampled	No. of communicating interfaces	95% confidence limits for number of communicating interfaces
		%	*n*	*r*	*R*
Control (edge)	449	3.03	33	32	12–14
(at random)	243	3.03	25	24	11–14
	257	2.19	28	27	12–14
	258	2.81	24	24	12–14
	259	2.82	39	36	11–14
Total		2.72‡	149	143	13–14‡
Regenerating	456a*	0.005	36	2	0.10–2.7
	573a*	0.007	79	4	0.20–1.8
	563a*	0.081	57	3	0.16–2.1
	451a*	0.067	13	1	0.00–5.1
	488	0.005	21	1	0.02–3.4
	451	0.009	13	2	0.27–6.5
	450	0.006	5	1	0.07–10.2
Total		0.029‡	224	14	0.46–1.46‡

The area of hepatocyte membranes and that of the gap junctions they include were obtained as indicated in Materials and Methods. The total membrane area examined was >5,000 μm^2 for control liver and 8,500 μm^2 for regenerating liver. A communicating interface is that contact face of one hepatocyte with a neighbor on which at least one gap junction is found. The actual number of communicating interfaces per hepatocyte was derived by noting that the probability of observing r communicating interfaces in n observations can be calculated using the binomial equation:

$$P(r) = \binom{n}{r} P^r (1 - P)^{n-r}$$

If $P(r)$ is allowed to take all the values between 0.05 and 0.95 (95% confidence interval, see reference 10), one can place bounds on P, the average frequency with which communicating interfaces do occur. Because the average interface seen in freeze-cleaved samples represents only 7% (see text) of the contact area of any hepatocyte, the actual number of communicating interfaces, R, assuming that they are uniformly distributed among hepatocytes, is: $R = (1/.07) P$. The last column gives the range of values obtained in normal and regenerating samples. R is not the same as the number of hepatocytes with which any one hepatocyte forms gap junctions.

* Indicates that the sample was also studied electrophysiologically.

‡ Average of listed values.

TABLE II

Resting Potentials in Normal and Regenerating Rat Liver

	Hours after partial hepatectomy	Membrane potential (mean ± S.E.M.)		No. of cells tested
		mV		
Controls		27 ± 1		26
		29 ± 0.3		46
		28 ± 0.7		46
		32 ± 0.8		58
		33 ± 0.5		40
		27 ± 0.6		20
		33 ± 0.4		67
		35 ± 1		9
	Average	31 ± 0.2	Total	312
Regenerates	31	47 ± 1		20
	33	46 ± 3		19
	31	37 ± 7		9
	32	40 ± 8		40
	32	46 ± .7		85
	32	46 ± 1		24
	32	46 ± 2		13
	Average	43 ± 0.3	Total	210

junctions and the incidence of coupling will be presented in Discussion.

IS COUPLING VIA THE EXTRACELLULAR SPACE: The studied by Furukawa and Furshpan (21) and Bennett and Trinkaus (6) demonstrated that electrical coupling can be mediated by a restricted extracellular space. To determine whether such a mechanism contributed to the electrical coupling of hepatocytes, we first impaled a pair of hepatocytes, then advanced either the current or voltage electrodes into the extracellular space between hepatocytes and remeasured the size of the coupling potential. Observation of a potential near 0 mV was used as a criterion for placing the electrodes in the extracellular space. Electrotonic coupling was observed only when both electrodes were in hepatocytes. This result was obtained with control and regenerating liver whether the current or voltage microelectrode was advanced into the extracellular space (Fig. 12). It therefore seems unlikely that the electrical coupling of hepatocytes is due to a restricted extracellular space (see also Fig. 6*b*).

DISCUSSION

Electrical measurements strongly suggest the presence of a low resistance pathway between adjacent hepatocytes in the rat liver. As Katz (31) has shown, in the absence of any surface membrane specialization, separation of small cells by as little as 150 Å virtually eliminates any intercellular spread of current. Because we have observed no evidence for coupling by way of

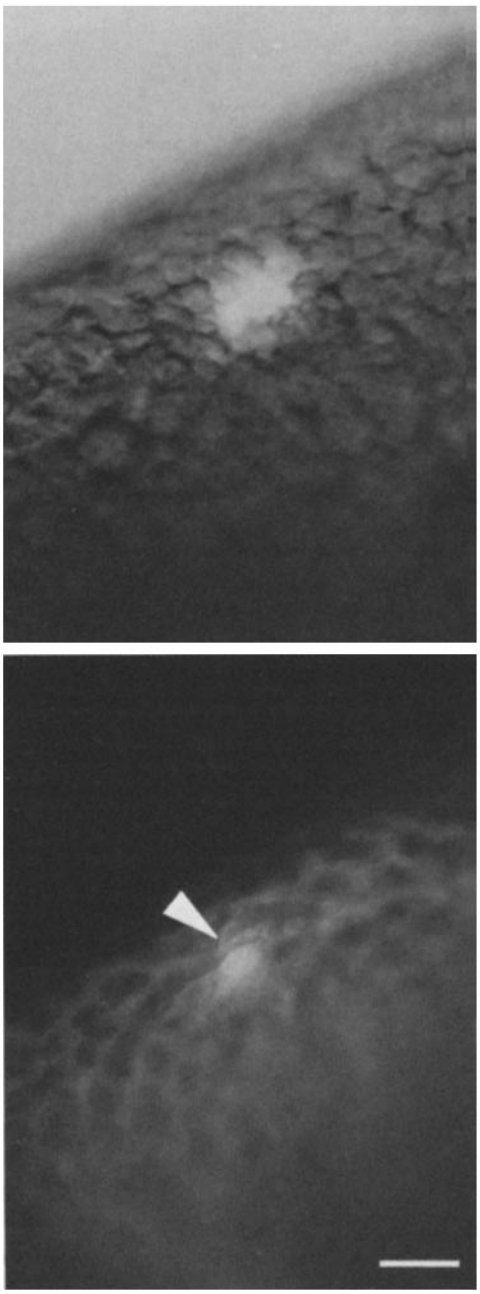

FIGURE 6 (a) Light micrograph showing spread of 6-carboxyfluorescein among hepatocytes in control rat liver. Dye was injected into a single hepatocyte ~3 min before this photograph was taken. The liver slice is shown transilluminated with visible light and from above with UV. Bar, 50 μm. (b) Extracellular spread of 6-carboxyfluorescein in control rat liver. A hepatocyte (arrow) was impaled with a dye-filled microelectrode. The microelectrode was then advanced into the extracellular space between hepatocytes (as signified by a potential of 0 mV at the electrode tip) and dye was ejected as usual. The photograph was taken within 1 min after beginning the injection. The cells are outlined by the dye, but dye does not enter cells. This specimen was illuminated only with UV. Bar, 50 μm.

a restricted extracellular space (Figs. 6*b* and 11), the extensive electrical coupling between hepatocytes implies the existence of a low resistance pathway between cell interiors (see also reference 42).

Our results from control liver are in reasonable agreement with those of previous studies of electrical communication between hepatocytes. Penn (42) obtained evidence for a low-resistance pathway for current flow between cells in mouse liver (see also reference 27). He found that the magnitude of electrotonic potentials was a linear function of the stimulus current. A similar result was obtained by Graf and Petersen (25). They also calculated values for Rm (5,050 Ω/cm^2) and Ri (1,360 Ω/cm) for mouse liver. The differences between their estimates and our own have at least two origins. First, there appear to be genuine differences in the properties of mouse and rat hepatocyte membranes because the size of electrotonic potentials at comparable interelectrode distances in mouse liver are smaller than in rat liver. Second, the mathematical model for the analysis of the spatial dependence of electrotonic potentials used by Graf and Petersen (25) was somewhat different than ours. Graf and Petersen used a planar model for the liver but did not describe the actual shape of their preparation. They also allowed the thickness of their preparation to be a free parameter in their model. Finally, they reported the presence of layers of uncoupled hepatocytes which we have never observed in rat liver.

Comparison of Communication in Normal and Regenerating Rat Liver

In our comparison of normal and regenerating liver we observed marked changes in intercellular communication. In normal liver every pair of hepatocytes impaled was found to be coupled (Table IV A) whereas in regenerating liver a variable number of pairs was found not to be coupled (Table IV B). Changes in the time-course and in the spatial dependence of electrotonic potentials in regenerating liver also suggest a substantial increase in the specific resistance Ri. This parameter reflects the combined resistance of hepatocyte cytoplasm and of the intercellular connections. Because the values of Ri

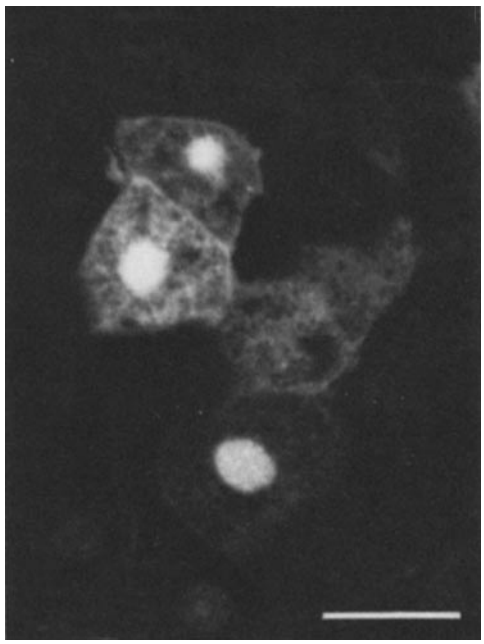

FIGURE 7 Thick section of regenerating liver showing several hepatocytes that are intracellularly stained with Lucifer Yellow. A single cell was injected initially and the dye was allowed to spread to several adjacent hepatocytes before fixation of the specimen. As has also been shown by others, the dye preserved after specimen preparation appears to have bound preferentially to cell nuclei. Bar, 20 μm.

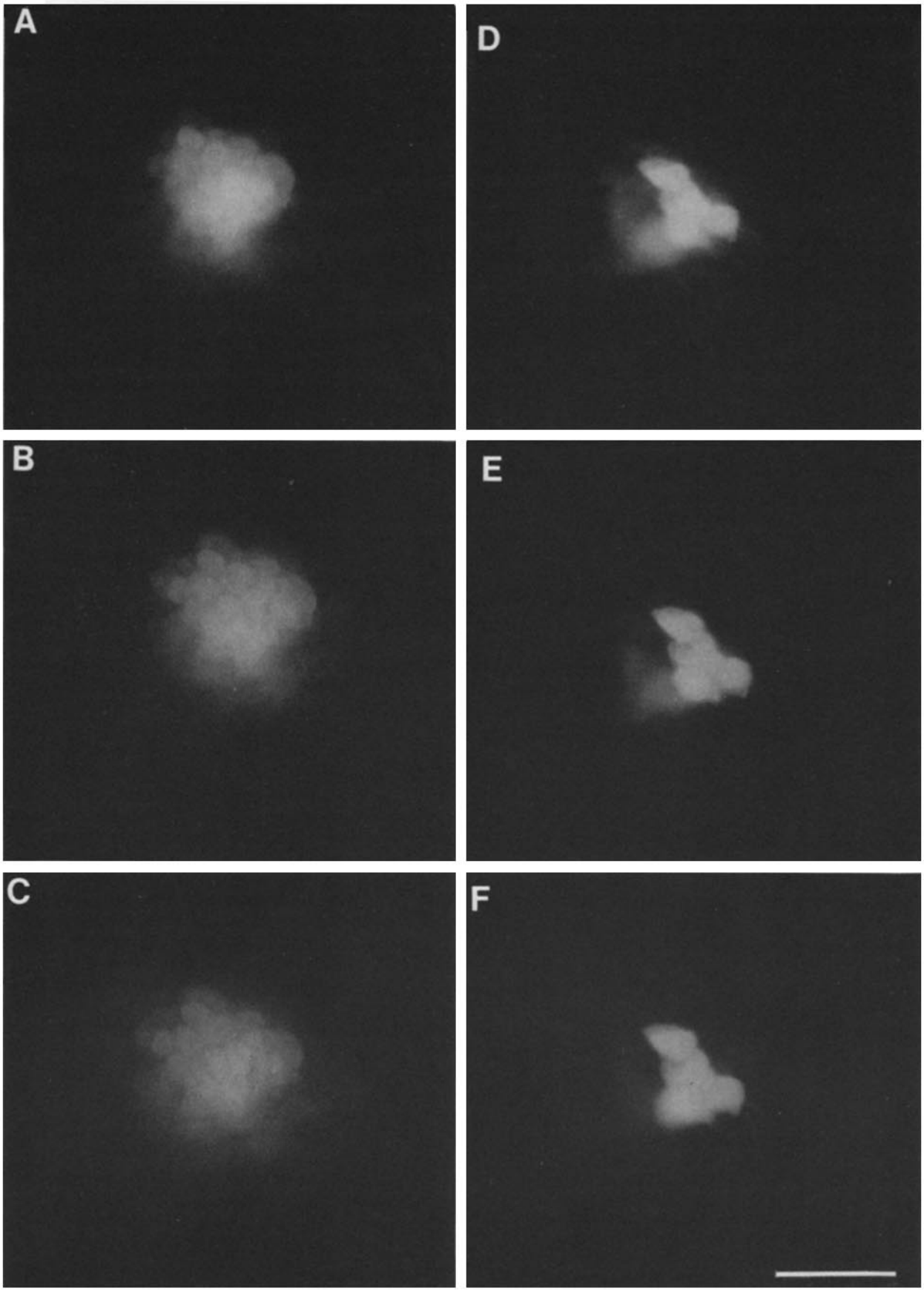

FIGURE 8 Dark-field photomicrographs comparing the spread of 6-carboxyfluorescein among hepatocytes in normal (*A–C*) and regenerating rat livers (*D–F*). In each sequence, dye was injected into a single hepatocyte iontophoretically for 30 s. Photomicrographs were taken immediately after the microelectrodes were withdrawn (*A* and *D*), 2 min (*B* and *E*), and 5 min later (*C* and *F*). Dye spread rapidly among hepatocytes in control liver (*A–C*). In contrast, in regenerating liver, dye spread only among a small group of hepatocytes. In regenerating liver, dye did not spread any farther after the completion of the injection (*D–F*). Bar, 40 μm.

for normal or regenerating liver are 1 to 2 orders of magnitude larger than commonly accepted values for cytoplasmic resistivity (31), we attribute the resistance increase observed in regenerating liver to increases in the resistance of the intercellular connections.

Marked differences between normal and regenerating liver were also seen when the spread of fluorescent dyes was examined. Both lucifer yellow and 6-carboxyfluorescein spread rapidly among hepatocytes when injected intracellularly in normal liver (Figs. 6 and 8). In regenerating liver, dye spread was much less extensive (Fig. 8). It should be noted that we cannot rule out the possibility of changes in intracellular binding or quenching of dye molecules in regenerating liver though we consider it unlikely that such effects can explain our results. Thus both the measurements of electrical coupling and the studies of dye spread imply decreases in the permeability of intercellular pathways in regenerating liver. These observations are consistent with two not mutually exclusive models: a decrease in the diameter of an intercellular channel (17, 50) or a decrease in the number of channels present between cells. As there are good reasons to believe that gap junctions represent aggregates of intercellular channels (37, 55) and because the number of these structures is dramatically reduced in regenerating liver, we favor the latter explanation.

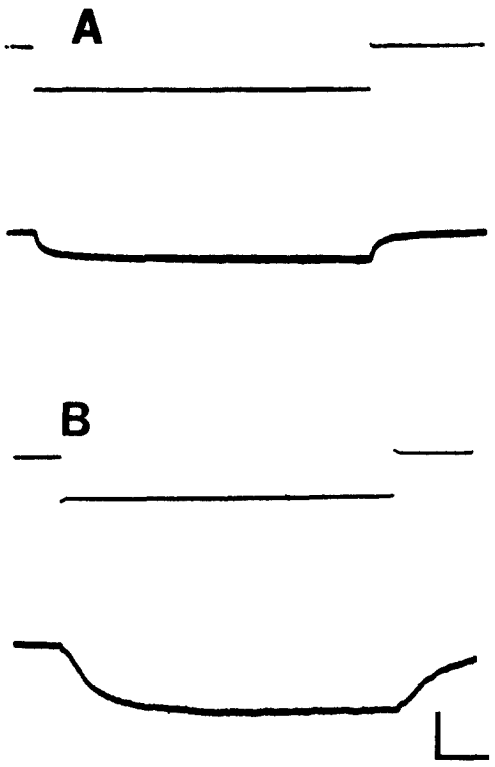

FIGURE 9 Electrotonic pulses observed in normal (*A*) and regenerating (*B*) liver. Current and voltage microelectrodes were separated by 50 μ and a 5×10^{-8} A test pulse was used. Upper trace in each panel is the output of the virtual ground circuit; lower trace is a recording of membrane potential. Vertical bar, 5×10^{-8} Å, 10 mV; Horizontal bar, 5 μm.

At first glance our results seem at odds with Loewenstein and Penn's previous investigations (35) of electrical coupling between hepatocytes in the regenerating adult liver where no differences were found. In adult rats, however, the time-course of gap junction disappearance is not as clear-cut and the extent of gap junction disappearance not as complete as in weanlings (61). Also, the earlier investigators did not examine coupling at times when the complement of gap junctions is minimal (61). Hence there is a reasonable explanation for the difference between our results and those of Loewenstein and Penn.

Analysis of the Distribution of Communicating Interfaces

It is instructive to compare the distribution of gap junctions with changes in electrical coupling more closely. The hypothesis that the connexons that comprise gap junctions represent the intercellular channels requires that there be a sufficient number of gap junctions per hepatocyte to account for the pattern of intercellular communication in normal and in regenerating rat liver. In normal liver virtually all hepatocyte membrane interfaces examined were communicating interfaces (Table I). We conclude that in normal liver each hepatocyte forms

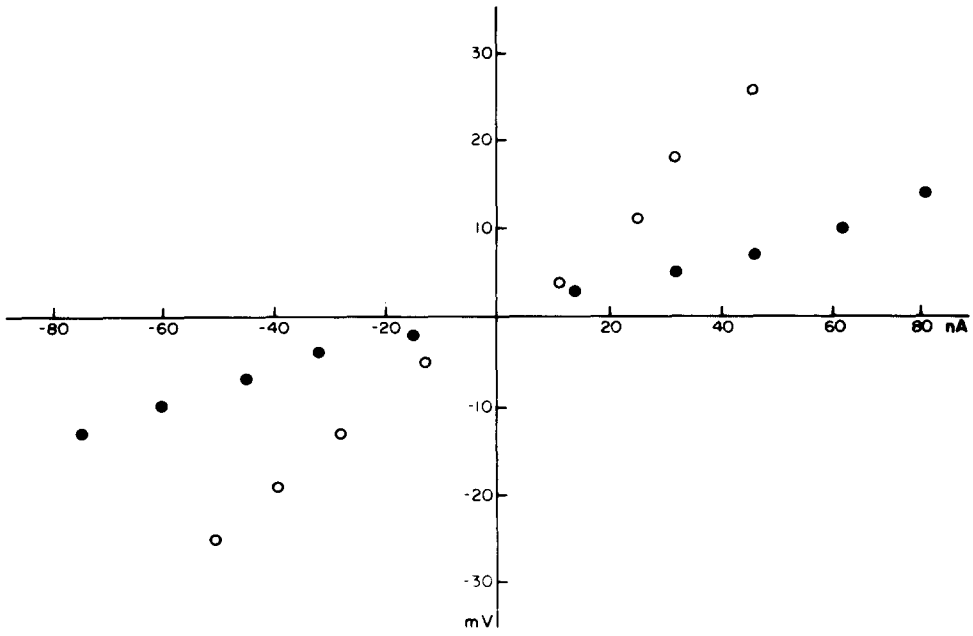

FIGURE 10 Current-voltage plots for control (●) and regenerating (○) liver. The amplitude of the electrotonic potential has been plotted as a function of the stimulus current. Current and voltage electrodes were separated by 50 μm. Each data point represents a single observation.

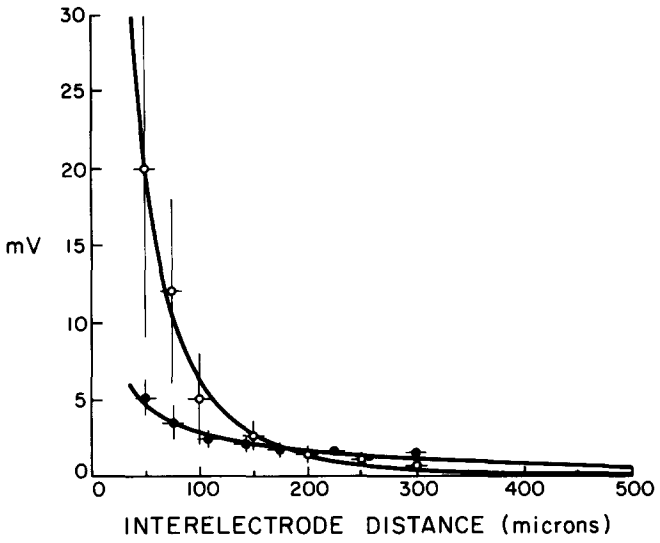

FIGURE 11 Spatial dependence of electrotonic potentials in control (●) and regenerating (○) liver. The amplitude of the electrotonic potential has been plotted as a function of the distance between current and voltage electrodes. A 5×10^{-8} A test pulse has been used. Each point is the mean of 3-21 measurements made with a single preparation; uncoupled cells have not been included in these calculations. Error bars are ±10 μm and ±1 SD of the mean electrotonic potential. The same data points have been fit with equation 1 (11A) and 2 (11B) as described in Table II.

TABLE III

Cable Analysis of Intercellular Communication in Liver

	Model 1		
	Rm (Ωcm^2)	Ri (Ωcm)	
Controls	16,245	2309	
	5,130	3499	
	8,356	3857	
	7,641	4225	
	10,859	3833	
	6,640	2750	
	9145 ± 1619	3412 ± 300	
			Hours after partial hepatectomy
Regenerates	17,009	42,337	33
	9,366	38,222	—
	11,339	45,456	32
	8,905	25,183	32
	21,615	33,965	35
	13,647 ± 2458	37,233 ± 3660	

Values of *Rm* and *Ri* were calculated using equation (23) from the appendix. Values of *Rm* and *Ri* that resulted in the best fit to our data were computed using a nonlinear least squares fitting program.

one or more gap junctions with the immediately adjacent cells. The widespread electrical coupling and extensive dye spread observed in normal liver are consistent with the distribution of gap junctions. In regenerating liver there appear to be only 1 or 2 communicating interfaces per hepatocyte (Table I). Because most hepatocyte pairs tested were coupled there should have been two or three communicating interfaces per hepatocyte at the minimum. Our analysis therefore suggests that there are too few communicating interfaces to account for the pattern

TABLE IV

Incidence of Coupling

No. of cell studied	No. of uncoupled cell pairs	No. of hours after partial hepatectomy at sacrifice
	A Regenerating Liver	
23	2	28.5
41	1	29.5
10	0	31.5
8	3	31.5
23	0	31.75
40	1	32.0
20	0	32.0
44	1	32.0
12	1	32.0
13	3	32.5
48	8	33.0
21	2	34.0
16	2	35.0
319	24	
	B Control Liver	
44	0	
35	0	
25	0	
42	0	
37	0	
60	0	
64	0	
7	0	
40	0	
354	0	

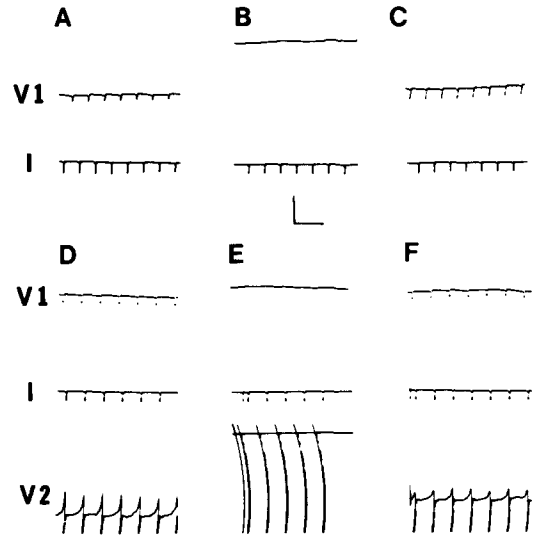

FIGURE 12 Electrical coupling of hepatocytes is not mediated by restricted extracellular space. In panel *A*, 2 microelectrodes were inserted into hepatocytes. Current pulses (5×10^{-8} A) were ejected from one (V_2; trace not shown) and the resulting electrotonic potentials were recorded by the other (V_1; top trace). The output of the current monitor is shown in the lower trace (I). In panel *B*, microelectrode V_1 has been advanced into the extracellular space between hepatocytes and then into the hepatocyte immediately beneath (panel *C*). Electrical coupling was observed only with both electrodes in hepatocytes. In panels *D-F* the experiment was repeated except that the current-passing microelectrode was advanced. Traces V_1 and I are as in *A-C*; V_2 is the potential at the tip of current-passing electrode; vertical bar represents 20 mV and 10^{-7} A; horizontal bar, 400 ms.

of intercellular communication in regenerating liver. There are several possible explanations for this apparent discrepancy.

First, we have assumed that hepatocytes behave as a uniform population during regeneration and therefore have used average values for the parameters considered in this analysis. However, it is known that hepatocytes are a heterogeneous population both metabolically and morphologically (cell size and organelle development). Subpopulations can be delineated both in normal and in regenerating liver that are, in general, related to position within the liver lobule (14, 47). Hepatocyte subpopulations most responsive to the proliferative stimulus after hepatectomy are those located near the periportal areas of the lobule. Hepatocytes nearest the terminal branches of the hepatic vein are less affected (47). One might expect that there is a similar inhomogeneity in the distribution of gap junctions and therefore of communicating interfaces among the subpopulations present in regenerating liver. A simple comparison of averaged morphological and physiological data may not be appropriate because we cannot be certain that the two techniques sample the populations equally.

A further possible source of error is that very small gap junctions might have been missed in our morphological studies. It is in fact reasonable to expect that a certain fraction of the gap junctions present in the regenerating liver went undetected. In 29- to 35-h regenerates, gap junctions were very small; some were made up of <10 particles or connexons. Such small junctions are sometimes difficult to identify, particularly in areas of E-face membrane where their presence is indicated only by pits. Junctions formed by single connexon pairs could also serve as intercellular channels but would be undetectable by our morphological techniques.

Is the Connexon the Intercellular Channel

A test of the idea that a connexon represents a single intercellular channel is to compare the change in the specific resistance, Ri, with the change in the area of gap junctions in normal and regenerating liver. One might expect the specific resistance, to vary inversely with the area of the junctions. Such a direct comparison requires that the pattern of current flow be similar in the two preparations. Otherwise, measurements of the specific resistance will be influenced to different degrees by other factors, such as the degree of branching in the electrical network and the tortuosity of current flow. There is good reason to believe that the pattern of current spread is very different in normal and regenerating liver. The absence of detectable coupling between some pairs of hepatocytes in regenerating liver (Table IV), the remarkably large variability in the size of electrotonic potentials in regenerating liver (Fig. 11) and the pattern of dye spread (Fig. 8) indicate that some hepatocyte interfaces are devoid of junctional channels in regenerating but not in normal liver. As a consequence, stimulus currents follow a tortuous pathway between current and voltage microelectrodes in regenerating liver, whereas in normal liver the pathway is more direct. Because of the tortuous nature of current flow the value of Ri computed from our data may not bear the same relationship to the number of connexons in regenerating as it does in normal liver. In regenerating liver the calculated value of Ri increases by ~10-fold (Table III). At the same time we find that the membrane area occupied by gap junctions is ~100-fold less than in normal liver (Table I). For the reasons just discussed, the apparent disagreement between the theory that each connexon represents a single patent intercellular channel and the experimental data is difficult to interpret. Matters are further complicated by the problems of detecting very small clusters of connexons, the possible heterogeneity in the distribution of gap junctions in regenerating liver (discussed previously), and the difference in density of hepatocyte surface membrane in normal and in regenerating liver. Thus, although one might be tempted to argue that our data show that connexons are not intercellular channels or that a certain fraction of the channels are closed in normal but not in regenerating liver, we feel that such a drastic revision of presently held views is unwarranted at this time. We emphasize that the observed changes are in the direction predicted by the theory that gap junctions are aggregates of intercellular channels.

A further test of the hypothesis that gap junctions are aggregates of intercellular channels is to combine our morphological and physiological data to estimate the conductance of one of these putative channels (a connexon). Studies of the permeation of intercellular channels by various probe molecules has led to the general impression that the intercellular channel has a diameter of 10 Å and a corresponding conductance of ~100 picosiemens (pS) (5, 33). It is clearly of interest to determine whether the conductance associated with a single connexon is consistent with this estimate.

We begin by considering the flow of current in normal rat liver. We assume that current flow through any one but the stimulated hepatocyte is one dimensional; that is, for a pair of neighboring hepatocytes, current flows only between opposing cell surfaces. Then the resistance due to one hepatocyte may be calculated from the relation: $R_h = R_i\, l/a$ where R_h is the resistance of an hepatocyte, l is the length, and a the area through which current flows. The appropriate dimensions are those of a hepatocyte because the model we use represents the liver as only two compartments: one extracellular and the other a smeared-out representation of hepatocyte cytoplasm and junctional membranes. Hence the resistance of a hepatocyte, including its junctional membranes, is calculated as the appropriate volume of this cytoplasmic compartment. If we represent hepatocytes as cubes ~17 μm on a side, then $R_h = 2 \times 10^6$. Because the specific resistance of the liver (Ri) is more than an order of magnitude greater than that of cytoplasm, we attribute the resistance R_h to the intercellular channels. The resistance of a hepatocyte (R_h) to a one-dimensional flow of current perpendicular to one of its surfaces is due to the channels between it and *one* of its neighbors. The number of connexons between a pair of hepatocytes is given by the product of the size of the contact area (100 μm^2), the percentage of contact area occupied by gap junctions (2.7%), and the density of connexons in a gap junction (11,000/μm^2), or ~29,000 connexons/interface. Because the connexons on one face are electrically in parallel, the resistance of one connexon is equal to the product of resistance of a hepatocyte (R_h) and the number of connexons per interface or $\sim 5 \times 10^{10}$ Ω; the conductance of a connexon is then estimated to be ~20 pS. This result is in reasonable agreement with the hypothesis that connexons are single intercellular channels. It should be noted that we have tacitly assumed in our calculations that each connexon is a patent or open channel although this has not been established. It should also be noted that we have omitted a similar calculation for regenerating liver. The reason is that we are less confident about our estimates of specific resistance in regenerating than in normal liver because of the tortuosity of current flow.

Could Other Structures be Responsible for Coupling

It is worth considering the possibility that structures other than gap junctions could mediate electrical coupling in the regenerating liver. Because there is good reason to believe that the intercellular pathway traversed by ionic current and dye molecules is insulated from the extracellular space (Figs. 6 and 12), whatever structure is proposed as an alternative to the gap junction must also form a continuous pathway between cell interiors. The only candidate for this role in the liver is the tight junction. The tight junction has never been shown to form an intercellular pathway, but it does represent sites of close contact between adjacent cells. Larsen et al. (32) have suggested the possibility that tight-junction-like structures might represent intercellular channels between partially communication competent cells. In the regenerating liver, although the number of gap junctions is greatly reduced, the tight junctions persist throughout the period of regeneration that we have studied (60, 62, and unpublished observations). Because uncoupled cell pairs of hepatocytes were observed throughout this period, it seems unlikely that tight junctions mediate intercellular communication in the liver. Another argument can be made from studies of the bullfrog sacculus. Because only tight junctions occur between the supporting cells and the hair cells (hair cells do not contact one another), the absence of electrical coupling between hair cells also implies that tight junctions do not mediate intercellular communication (A. J. Hudspeth, personal communication.).

Some investigators have considered the possibility that structures besides the gap junction mediate electrical coupling between cells either because gap junctions could not be demonstrated in the tissue or because the number of gap junctions present appeared to be too small to mediate the observed coupling (11, 22, 23, 53). The results of our analysis demonstrate that great care must be taken in attempting to compare the distribution of gap junctions with either the extent or the efficacy of electrical coupling. The origin of the disparity between the morphological and physiological data in this study is more likely to be in the simplifications in our analysis and the difficulty in detecting small numbers of connexons in regenerating liver than in a defect in the hypothesis that gap junctions are aggregates of intercellular channels. We believe that at the present time there is no compelling evidence that any other structure serves as a low-resistance pathway between cell interiors, though a proof of this is still lacking.

CONCLUSIONS

The biological significance of the reduction in the complement of gap junctions during liver regeneration remains enigmatic. The changes in intercellular communication that we have observed would be consistent with the hypothesis that such changes play a central role in the control of cell proliferation (33), although the actual mechanism is not at all evident. Another possibility is that the changes in coupling between restricted populations of hepatocytes could serve as a positional cue in the reorganization of liver architecture in a manner analogous to that suggested by Wolpert (58) for embryonic systems. Finally, the changes in gap-junction size and number may reflect alterations in the metabolic state of hepatocytes during a period of intense synthetic activity (8).

We conclude that there are qualitative and quantitative changes in intercellular communication in the regenerating rat liver at times when gap junctions are relatively rare. These changes are consistent with the suggestion that the connexons that comprise the gap junction are low-resistance channels between the interiors of adjacent cells although our observations did not allow a decisive test of this hypothesis.

We thank Jean Edens for help with the surgery. Jim Hudspeth and David Corey helped with the design of the equipment. Jim Hudspeth, Jerry Pine, and Bruce Nicholson made useful comments concerning the analysis and discussion of our results.

David Meyer and Barbara Yancey were supported by National Institutes of Health postdoctoral fellowships (NS 06240 and AM 05700). Our laboratory has also been supported by grants RR 07003 and GM 06965 from the NIH and by funds from the Northwest Foundation.

APPENDIX

Electrical Potential in a Wedge-Shaped Syncytium

ARTHUR PESKOFF

Departments of Physiology and Biomathematics, University of California, Los Angeles, California 90024

The problem of calculating the electric potential induced by a point source of current inside a syncytium has been formulated and solved for an unbounded syncytium (29, 43), for a syncytium bounded by two parallel planes (25), and for spherical (43) and cylindrical (44) syncytia.

The appropriate geometry for the liver measurements is a wedge-shaped syncytium. If the wedge angle is π/P radians, where P is an integer, the potential can be obtained most simply using the method of images, together with the known solution for the unbounded case. The number of image sources required is $2P - 1$. (In the case of two parallel planes, which is equivalent to a wedge angle of zero, or to $P = \infty$, an infinite number of images is required, as found by Graf and Peterson [25].) For the present case the wedge angle is 30° and consequently eleven images are needed.

Microelectrode measurements (see Results) fail to detect electrotonic potentials in the extracellular space of the liver. We therefore simplified the theoretical problem by omitting treatment of potential gradients in the extracellular space. This allows us to formulate the intracellular potential in terms of a

single partial differential equation (as in reference 29) rather than in terms of a pair of coupled partial differential equations (as in reference 43).[1]

In the present, simpler formulation, each hepatocyte is assumed to be in contact with the extracellular space which is at a constant potential $V_e = 0$. If the potential within an individual hepatocyte located at position $\vec{r}$ at time t is $V_i(\vec{r}, t)$ volts, then the current density in A/cm^2 crossing its membrane from the cell interior to the adjacent extracellular space is related to the voltage across the membrane by

$$J_m = \frac{V_i - V_e}{R_m} + C_m \frac{\partial}{\partial t}(V_i - V_e) = \frac{V_i}{R_m} + C_m \frac{\partial V_i}{\partial t} \qquad (1)$$

where R_m is the membrane resistance in ohm-cm^2 and C_m the membrane capacitance in farads/cm^2.

If there are χ square centimeters of hepatocyte membrane per cubic centimeter of liver, then there is a current χJ_m mA/cm^3 leaving the hepatocytes and entering the extracellular space. The divergence of the intracellular current density $\vec{J}_i$ is the current injected from the source I_0 at position $\vec{r}_0$, minus the membrane current per unit volume:

$$\nabla \cdot \vec{J}_i = I_0 \delta(\vec{r} - \vec{r}_0) - \chi J_m \qquad (2)$$

where $\delta(\vec{r} - \vec{r}_0)$ is a three-dimensional Dirac delta function.

It should be noted that in the present electrical model (29, 43) the actual membrane current, which crosses the boundary of each cell, is replaced by an equal amount of fictitious, smeared-out current, which is assumed to exist throughout the liver volume.

The corresponding assumption for modeling current flow from cell to cell through the gap junctions assumes that the interiors of all the coupled hepatocytes behave as a single medium with effective resistivity R_i ohm-cm. R_i is determined principally by the resistance and spatial distribution of the individual junctions and is much larger than the resistivity of the medium within a single cell. The actual intracellular potential is therefore relatively constant within a single cell (except near the current microelectrode), most of the change in potential occurring across the cell-to-cell junctions; the potential in the model will vary smoothly throughout space and will not display the abrupt changes from cell to cell. Ohm's law for the intracellular current is thus

$$\vec{J}_i = -\frac{1}{R_i} \nabla V_i \qquad (3)$$

where $-\nabla V_i$, the negative gradient of the potential, is the intracellular electric field.

This model should describe the potential accurately for electrode separations large compared to the dimensions of a single cell, but be subject to more statistical variations from sample to sample for smaller distances. The validity of the theory for all distances is improved, however, by averaging the potential measurements over many samples. That is, the model should be better at predicting the expectation value of the potential than it is at predicting an individual potential measurement, which is affected by a specific sample configuration of cells. It would, of course, require a more complicated theory to make any quantitative statements about the statistics of the variations from sample to sample.

Taking the divergence ($\nabla \cdot \vec{J}_i$) of Eq. (3), equating it to Eq. (2) and substituting Eq. (1) for J_m yields the partial differential equation

$$\frac{1}{R_i} \nabla^2 V_i - \frac{\chi V_i}{R_m} - \chi C_m \frac{\partial V_i}{\partial t} = -I_0 \delta(\vec{r} - \vec{r}_0) \qquad (4)$$

for the intracellular potential, where $\nabla^2 = \nabla \cdot \nabla$ is the Laplacian operator.

We now need the boundary condition that V_i must satisfy at the surface of the liver. The component of current density normal to the surface of the liver is given by the component of Eq. 3 in the direction perpendicular to the surface, $-(1/R_i)\partial V_i/\partial n$, where $\partial/\partial n$ denotes the normal derivative in the outward direction. Equation 1, for the outer membranes, yields the boundary condition.

$$-\frac{1}{R_i}\frac{\partial V_i}{\partial n} = \frac{V_i}{R_m} + C_m \frac{\partial V_i}{\partial t} \quad \textit{at the surface} \qquad (5)$$

In Eq. 5 it is assumed that the surface membranes have the same electrical properties (R_m and C_m) as the inner membranes and that Glisson's capsule, which partly surrounds the liver (the capsule was incised during dissection), contributes negligible additional electrical impedance. The latter assumption is suggested by microelectrode measurements that found no detectable voltage drop between the extracellular space within the liver and the bath.

It is assumed that before $t = 0$, the system is quiescent, so that

$$V_i = 0 \quad \text{at} \quad t = 0 \qquad (6)$$

We now write Eqs. 4 and 5 in nondimensional form. This procedure will identify a small parameter, ϵ, multiplying the nondimensional potential and its time derivative at the surface and thereby permit a great simplification in the boundary condition. Defining the space constant λ and time constant τ by

$$\lambda^2 = \frac{R_m}{\chi R_i}; \quad \tau = R_m C_m \qquad (7)$$

the dimensionless distance and time variable by

$$\vec{R} = \frac{\vec{r}}{\lambda}; \quad T = \frac{t}{\tau} \qquad (8)$$

the dimensionless potential by

$$\Phi = \frac{4\pi\lambda V_i}{I_0 R_i} \qquad (9)$$

and a dimensionless parameter ϵ by

$$\epsilon = \frac{\lambda R_i}{R_m} = \frac{1}{\chi\lambda} = \sqrt{\frac{R_i}{R_m \chi}} \qquad (10)$$

equations (4), (5), and (6) become

$$\nabla_R^2 \Phi - \Phi - \frac{\partial \Phi}{\partial T} = -4\pi\delta(\vec{R} - \vec{R}_0) \qquad (11)$$

[1] Doing this ignores terms of order R_e/R_i, the ratio of effective extracellular resistivity, to effective intracellular resistivity. A perturbation analysis of the coupled partial differential equations can be done, by expanding the potentials in powers of the small parameter R_e/R_i. In this way it can be shown that the error introduced in the intracellular potential using the simpler formulation is comparable to the total extracellular potential, which for our purposes is negligible. The perturbation analysis will not be included here.

$$\frac{\partial \Phi}{\partial N} + \epsilon\left(\Phi + \frac{\partial \Phi}{\partial T}\right) = 0 \quad \textit{at the surface} \tag{12}$$

$$\Phi = 0 \quad \text{at} \quad t = 0 \tag{13}$$

$\nabla_R{}^2$ and $\partial\Phi/\partial N$ denote the Laplacian and normal derivative with respect to the nondimensional spatial coordinates. To obtain Eq. 11 we have used the relation

$$\delta(\vec{r} - \vec{r}_0) = \delta(\lambda\vec{R} - \lambda\vec{R}_0) = \lambda^{-3}\delta(\vec{R} - \vec{R}_0)$$

Substituting $R_i = 3 \times 10^3$ Ω-cm, $R_m = 9 \times 10^3$ Ω-cm^2, $\chi = 3 \times 10^3$ cm^{-1} for normal liver, or $R_i = 3 \times 10^4$ Ω-cm, $R_m = 1.7 \times 10^4$ Ω-cm^2, $\chi = 5 \times 10^3$ cm^{-1} for regenerating liver yields $\epsilon \sim 10^{-2} \ll 1$. If we let ϵ equal zero in the boundary condition Eq. 12 we obtain the simpler boundary-value problem

$$\nabla_R{}^2\Phi_0 - \Phi_0 - \frac{\partial \Phi_0}{\partial T} = -4\pi\delta(\vec{R} - \vec{R}_0)$$

$$\frac{\partial \Phi_0}{\partial N} = 0 \quad \textit{at the surface} \tag{14}$$

$$\Phi_0 = 0 \quad \text{at} \quad t = 0$$

where the error in using Φ_0 in place of Φ is of order $\epsilon \sim 10^{-2}$. This can be justified rigorously by a formal perturbation analysis in which Φ_0 is the leading term in a perturbation expansion of Φ, of the form $\Phi = \Phi_0 + \epsilon\Phi_1 + \epsilon^2\Phi_2 + \ldots$, as has been done in the analysis of potential in a spherical cell (45). (Because of the closed boundary in the spherical cell, there was an additional ϵ^{-1} term, which does not appear in the wedge geometry because of the open boundary.) The boundary condition in Eq. 14 indicates that in the approximation used here, there is no current crossing the outer surface of the liver.

Dropping the second and third term in the boundary condition Eq. 12, which represents current crossing the outer surface, but retaining the second and third term in the partial differential equation (Eq. 11), which represents current crossing the internal membranes, can be justified also on physical grounds. The current leaves the liver in a volume of order λ^3 around the current source, via total areas $\chi\lambda^3$ of internal membrane and, at most, λ^2 of surface membrane. Consequently, the ratio of surface to internal area in this volume, $1/\chi\lambda = \epsilon$, is small, and the surface current portion can be neglected.

Before using the method of images for a wedge-shaped tissue, we need the solution to an unbounded tissue, with the source located at the origin of coordinates, that is, the solution to

$$\nabla_R{}^2\Phi - \Phi - \frac{\partial \Phi}{\partial T} = -4\pi\delta(\vec{R})$$

$$\Phi \to 0 \quad \text{as} \quad R \to \infty \tag{15}$$

$$\Phi = 0 \quad \text{at} \quad t = 0$$

where $R = |\vec{R}|$ is the radial coordinate in a spherical coordinate system with origin at the source point. The solution to Eq. 15 is (29)

$$\Phi(\vec{R}, T) = \frac{e^{-R}}{2R}\operatorname{erfc}\left(\frac{R}{2\sqrt{T}} - \sqrt{T}\right) + \frac{e^{R}}{2R}\operatorname{erfc}\left(\frac{R}{2\sqrt{T}} + \sqrt{T}\right) \tag{16}$$

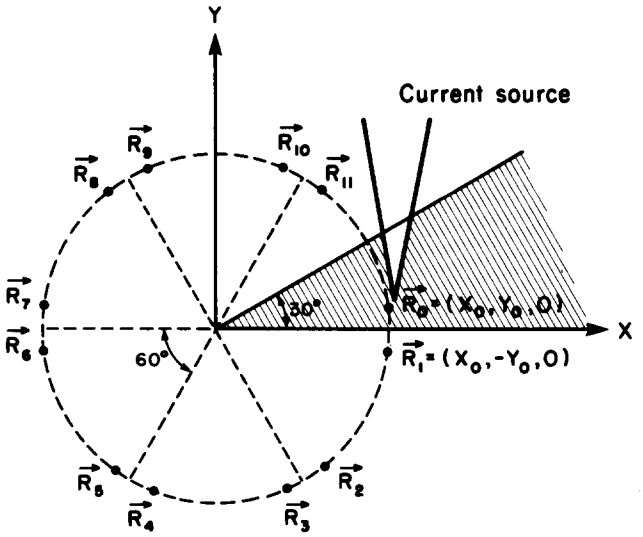

FIGURE 13 Diagram showing the location of the real ($\vec{R}_0$) and image sources ($\vec{R}_1 - \vec{R}_{11}$) for the cable analysis of current spread in the liver. The liver is depicted as the cross-hatched region.

and the steady-state response, which is the limit of Eq. 16 as $T \to \infty$, is

$$\Phi(\vec{R}, T = \infty) = \frac{e^{-R}}{R} \tag{17}$$

We now assume that the liver is a wedge-shaped tissue with a 30° angle as shown in Fig. 13. The tissue is assumed of infinite extent in the X and Z direction, where the Z-axis, the intersection of the two planar surfaces, is directed perpendicular to and out of the plane of the figure. This is justified because the actual dimensions are much greater than the space constant λ, which is a measure of the spatial extent of the electric potential.

Using the method of images, the solution to Eq. 14 can be obtained as a sum over terms of the form of Eq. 16, with R replaced by the various distances to the source and to the images. The locations of the images are shown in Fig. 13 for a 30° wedge with a source located at $\vec{R}_0 = (X_0, Y_0, 0)$.

The first image point is located at $\vec{R}_1 = (X_0, -Y_0, 0)$, the reflection of the source point in the X,Z-plane. The remaining images are located by successive rotations of $\vec{R}_0$ and $\vec{R}_1$ through an angle of 60° clockwise. Thus, the other image locations are related to $\vec{R}_0$ and $\vec{R}_1$ by

$$\vec{R}_{p+2} = \left(X_p\cos\frac{\pi}{3} + Y_p\sin\frac{\pi}{3}, -X_p\sin\frac{\pi}{3} + Y_p\cos\frac{\pi}{3}, 0\right) = \left(\frac{1}{2}X_p + \frac{\sqrt{3}}{2}Y_p, -\frac{\sqrt{3}}{2}X_p + Y_p, 0\right); \quad p = 0, 1, 2, 3, 4 \tag{18}$$

and the solution to Eq. 14 for the potential at a point (X, Y, Z) at time T inside the wedge is

$$\Phi_0(\vec{R}, T) = \sum_{k=0}^{11}\left[\frac{e^{-|\vec{R} - \vec{R}_k|}}{2|\vec{R} - \vec{R}_k|}\operatorname{erfc}\left(\frac{|\vec{R} - \vec{R}_k|}{2\sqrt{T}}\sqrt{T}\right) + \frac{e^{|\vec{R} - \vec{R}_k|}}{2|\vec{R} - \vec{R}_k|}\operatorname{erfc}\left(\frac{|\vec{R} - \vec{R}_k|}{2\sqrt{T}} + \sqrt{T}\right)\right] \tag{19}$$

which in the steady state, $T \to \infty$, is

$$\Phi_0(\vec{R}, T = \infty) = \sum_{k=0}^{11} \frac{e^{-|\vec{R} - \vec{R}_k|}}{|\vec{R} - \vec{R}_k|} \tag{20}$$

where $|R - \vec{R}_k| = \sqrt{(X - X_k)^2 + (Y - Y_k)^2 + Z^2}$.

For the arrangement of source and image points in Fig. 13, it is seen that for each point below the X,Z-plane there is a symmetrically placed point above the X,Z-plane. Consequently, the electric field component normal to the X,Z-plane, or $\partial\Phi_0/\partial N$, is zero. Similarly, there is a symmetric pairing of points with respect to the 30° plane. Therefore, $\partial\Phi_0/\partial N = 0$ on both planes, as required.

In the more general case when the wedge angle is π/P, P an integer, with a source at $\vec{R}_0 = (X_0, Y_0, 0)$, the first image is again at $\vec{R}_1 = (X_0, -Y_0, 0)$ and the other $2P - 2$ images are located by successive rotations of $\vec{R}_0$ and $\vec{R}_1$ through an angle $2\pi/P$ or

$$\vec{R}_{p+2} = \left(X_p \cos\frac{2\pi}{P} + Y_p \sin\frac{2\pi}{P}, -X_p \sin\frac{2\pi}{P} + Y_p \cos\frac{2\pi}{P}, 0\right); \quad p = 0, 1, 2, \ldots 2P - 1 \tag{21}$$

and the transient and steady-state potentials are given by Eqs. (19) and (20) with the index k going from 0 to $2P - 1$.

If the wedge angle is not π/P, P an integer, the steady-state solution to the boundary-value problem can be obtained in the form of an infinite sum of Fourier cosine integrals of modified Bessel functions. The transient solution can be expressed as an inverse Laplace transform of the steady-state solution. The potential distribution around a point current source for a wedge angle of 33°, for example, would require a much more complicated computation, but it would be expected to lie between the solutions obtained by the image method for 30° and 36°, which require 11 and 9 images, respectively. A preliminary examination of this solution, however, indicates that a fit to the solution for a wedge of angle $\Theta \neq \pi/6$ rather than to the solution for $\pi/6$, would yield essentially the same value for λ, but R_i would be multiplied by $6\Theta/\pi$.

Expressing Eqs. (19) and (20) in terms of physical units, the intracellular potential at position $\vec{r} = (x, y, z)$ and time t is, using Eqs. (7), (8), and (9),

$$V_i(x, y, z, t) = \frac{I_0 R_i}{8\pi} \sum_{k=0}^{11} \left[\frac{e^{-|\vec{r} - \vec{r}_k|/\lambda}}{|\vec{r} - \vec{r}_k|} \operatorname{erfc}\left(\frac{|\vec{r} - \vec{r}_k|}{2\lambda\sqrt{t/\tau}} - \sqrt{\frac{t}{\tau}}\right) + \frac{e^{|\vec{r} - \vec{r}_k|/\lambda}}{|\vec{r} - \vec{r}_k|} \operatorname{erfc}\left(\frac{|\vec{r} - \vec{r}_k|}{2\lambda\sqrt{t/\tau}} + \sqrt{\frac{t}{\tau}}\right)\right] \tag{22}$$

and the steady-state intracellular potential is

$$V_i(x, y, z, t = \infty) = \frac{I_0 R_i}{4\pi} \sum_{k=0}^{11} \frac{e^{-|\vec{r} - \vec{r}_k|/\lambda}}{|\vec{r} - \vec{r}_k|} \tag{23}$$

where $|\vec{r} - \vec{r}_k| = \sqrt{(x - x_k)^2 + (y - y_k)^2 + z^2}$.

Dr. Peskoff was supported by National Institutes of Health Research Career Development Award No. 5K04 GM 00222-05 from the National Institutes of General Medical Sciences.

Received for publication 3 April 1981, and in revised form 16 July 1981

REFERENCES

1. Anderson, E. A., D. F. Albertini, and R. F. Wilkinson. 1977. Cytological differentiation of the female gamete. *In* International Cell Biology. B. R. Brinkley and K. R. Porter, editors. 561–568.
2. Barr, L., M. M. Dewey, and W. Berger. 1965. Propagation of action potentials and the structure of the nexus in cardiac muscle. *J. Gen. Physiol.* 48:797–823.
3. Barr, L., W. Berger, and M. M. Dewey. 1968. Electrical transmission at the nexus between smooth muscle cells. *J. Gen. Physiol.* 51:347–368.
4. Bennett, M. V. L. 1973. Permeability and structure of electrotonic junctions and intercellular movement of tracers. *In* Intracellular Staining in Neurobiology. S. B. Kater and C. R. Nicholson, editors. Springer-Verlag. 115–134.
5. Bennett, M. V. L. 1977. Electrical transmission: a functional analysis and comparison to chemical transmission. *In* Handbook of Physiology, Section 1, The Nervous System, Vol. 1. E. R. Kandel, J. M. Brookhart, and V. B. Mountcastle, editors. *Amer. Physiol. Soc.* 357–415.
6. Bennett, M. V. L., and J. P. Trinkaus. 1970. Electrical coupling of embryonic cells by way of extracellular space and specialized junctions. *J. Cell Biol.* 44:592–610.
7. Brink, P., and M. M. Dewey. 1978. Nexal permeability to anions. *J. Gen. Physiol.* 72:67–86.
8. Bucher, N. 1963. Regeneration of mammalian liver. *Int. Rev. Cytol.* 15:245–300.
9. Claret, M., and E. Coraboeuf. 1970. Membrane potential of perfused and isolated rat liver. *J. Physiol. (Lond.).* 210:137–138P.
10. Colquohoun, D. 1971. Lectures on Biostatistics. Oxford University Press, Oxford, England.
11. Daniel, E. E., V. P. Daniel, G. Duchon, R. E. Garfield, M. Nicholls, S. K. Malhotra, and M. Oki. 1976. Is the nexus necessary for cell to cell coupling of smooth muscle. *J. Membr. Biol.* 28:207–239.
12. Dewey, M. M., and L. Barr. 1964. A study of the structure and distribution of the nexus. *J. Cell Biol.* 23:553–584.
13. Dreifuss, J. J., L. Girardier, and W. G. Forssmann. 1966. Etude de la propagation de l'excitation dans la ventricule de rat au moyen de solutions hypertoniques. *Pfluegers Archiv. Gesamte Physiol. Menschen Tiere.* 292:13–33.
14. Drochmans, p., J. C. Wanson, C. May, and D. Bernaert. 1978. Ultrastructural and metabolic studies of isolated and cultured hepatocytes. *In* Hepatotrophic Factors. R. Porter and J. Whelan, editors. Elsevier Excerpta Medica, North Holland, 7–24.
15. Elias, H., and J. C. Sherrick. 1969. Parenchyma. *In* Morphology of the Liver. Academic Press, Inc., New York. 5–20.
16. Eves, H. 1975. Analytic geometry. *In* Handbook of Mathematical Sciences Sed. W. H. Beyer, editor. CRC Press, W. Palm Beach, Florida. p. 500.
17. Flagg-Newton, J., and W. Loewenstein. 1979. Experimental depression of junctional membrane permeability in mammalian cell culture. A study with tracer molecules in the 300–800-dalton range. *J. Membr. Biol.* 50:65–100.
18. Friedman, N., A. V. Somlyo, and A. P. Somlyo. 1973. Cyclic adenosine and guanosine monophosphates and glucagon: effect on liver membrane potentials. *Sciences N.Y.* 171: 400–402.
19. Fry, G., C. E. Devine, and G. Burnstock. 1977. Freeze fracture studies of nexuses between smooth muscle cells. Close relationship to sarcoplasmic reticulum. *J. Cell Biol.* 72:26–34.
20. Furshpan, E. J., and D. D. Potter. 1968. Low resistance junctions between cells in embryos and tissue culture. *Curr. Top. Dev. Biol.* A. A. Moscona, and A. Monroy, editors.
21. Furukawa, T., and E. J. Furshpan. 1963. Two inhibitory mechanisms in the Mauthner neurons of the goldfish. *J. Neurophysiol.* 26:140–176.
22. Gabella, G. 1972. Intercellular junctions between circular and longitudinal intestinal muscle layers. *Z. Zellforsch. Microsc. Anat.* 125:191–199.
23. Gabella, G., and D. Blundell. 1979. Nexuses between the smooth muscle cells of the guinea pig ileum. *J. Cell Biol.* 82:239–247.
24. Gilula, N. B., O. R. Reeves, and A. Steinbach. 1972. Metabolic coupling, ionic coupling and cell contacts. *Nature (Lond.).* 235:262–265.
25. Graf, J., and O. H. Petersen. 1978. Cell membrane potential and resistance in liver. *J. Physiol. (Lond.).* 284:105–126.
26. Goodenough, D. A. 1976. The structure and permeability of isolated hepatocyte gap junctions. Cold Spring Harbor Symp. Quant. Biol. XL. Cold Spring Harbor Laboratories, New York. 37–43.
27. Haylett, D. G., and D. H. Jenkinson. 1972. Effects of noradrenaline on potassium efflux, membrane potential and electrolyte levels in tissue slices prepared from guinea pig liver. *J. Physiol. (Lond.).* 225:721–750.
28. Hudspeth, A. J., and D. P. Corey. 1979. Controlled bending of high resistance electrodes. *Am. J. Physiol.* 234:C56–C57.
29. Jack, J. J. B., D. Noble, and R. W. Tsien. 1975. *In* Electric Current Flow in Excitable Cells. Oxford University Press, Oxford.
30. Johnson, R. G., M. Hammer, J. D. Sheridan, and J.-P. Revel. 1974. Gap junction formation between reaggregated Novikoff hepatoma cells. *Proc. Natl. Acad. Sci. U. S. A.* 71:4356–4540.
31. Katz, B. 1966. *In* Nerve Muscle and Synapse. McGraw Hill, New York.
32. Larsen, W. J., R. Azarnia, and W. R. Loewenstein. 1977. Intercellular communication and tissue growth; IX. Junctional membrane structure of hybrids between communication-competent and communication-incompetent cells. *J. Membr. Biol.* 34:39–54.
33. Loewenstein, W. R. 1979. Junctional intercellular communication and the control of growth. *Biochim. Biophys. Acta.* 560:1–65.
34. Loewenstein, W. R., and Y. Kanno. 1964. Studies on an epithelial (gland) cell junction I. Modifications of surface membrane permeability. *J. Cell Biol.* 22(2, Pt. 2):565 *a* (Abstr.).
35. Loewenstein, W. L., and R. D. Penn. 1967. Intercellular communication and tissue growth. II Tissue regeneration. *J. Cell Biol.* 33:235–242.
36. Luft, J. H. 1973. Embedding media—old and new. *In* Advanced Techniques in Biological Electron Microscopy. J. K. Koehler, editor. Springer-Verlag, Berlin. 1–34.
37. Makowski, L., D. Caspar, W. C. Phillips, and D. A. Goodenough. 1977. Gap junction structures II. Analysis of the X-ray diffraction data. *J. Cell Biol.* 74:629–645.
38. Meyer, D. J., S. B. Yancey, and J.-P. Revel. 1979. Electrotonic coupling and dye spread after disappearance of gap junctions. *J. Cell Biol.* 83(2, Pt. 2):312 *a* (Abstr.).
39. Motta, P., and K. R. Porter. 1974. Structure of rat liver sinusoids as revealed by scanning electron microscopy. *Cell Tissue Res.* 148:111–125.
40. Motta, P., M. Mato, and T. Fujita. 1978. The Liver. *In* An Atlas of Scanning Electron Microscopy. Igaku Shoin, Ltd., Tokyo.
41. Pappas, G. D., Asada, Y., and Bennett, M. V. L. 1971. Morphological correlates of increased coupling resistance at an electronic synapse. *J. Cell Biol.* 49:173–188.
42. Penn, R. D. 1966. Ionic communication between liver cells. *J. Cell Biol.* 29:171–174.
43. Peskoff, A. 1979. Electric potential in three-dimensional electrically syncytial tissues. *Bull. Math. Biol.* 41:163–181.
44. Peskoff, A. 1979. Electric potential in cylindrical scyncytia and muscle fibers. *Bull Math. Biol.* 41:183–192.
45. Peskoff, A., and Eisenberg, R. S. 1975. The time dependent potential in a spherical cell using matched asymptolic expansions. *J. Math. Biol.* 2:277–300.
46. Potter, D. D., E. J. Furshpan, and E. S. Lennox. 1966. Connections between cells in the developing squid as revealed by electrophysiological methods. *Proc. Natl. Acad. Sci. U. S. A.* 55:328.
47. Rabes, H. M. 1978. Kinetics of hepatocellular proliferation as a function of the microvas-

cular structure and functional state of the liver. *In* Hepatotrophic Factors. R. Porter and J. Whelan, editors. Elsevier Excerpta Medica, North Holland.
48. Revel, J.-P., S. B. Yancey, D. J. Meyer, and M. E. Finbow. 1980. Behavior of gap junctions during liver regeneration. Falk Symposium. *In* Communications of Liver Cells, F. Gudat and W. Reutter, editors. MTP Press Ltd., Lancaster.
49. Revel, J.-P., A. G. Yee, and A. J. Hudspeth. 1971. Gap junctions between electrotonically coupled cells in tissue culture and in brown fat. *Proc. Natl. Acad. Sci. U. S. A.* 68:2924–2927.
50. Rose, B., I. Simpson, and W. R. Loewenstein. 1977. Calcium ion produces graded changes in permeability of membrane channels in cell junction. *Nature* (*Lond.*). 267:625–627.
51. Schanne, O., and E. Coraboeuf. 1966. Potential and resistance measurements of rat liver cells *in situ*. *Nature* (*Lond.*). 210:1390–1391.
52. Sheridan, J. D. 1971. Electrical coupling between fat cells in the newt fat body and mouse brown fat. *J. Cell Biol.* 45:795–803.
53. Sheridan, J. D. 1978. Junction formation and experimental modification. *In* Intercellular Junctions and Synapses. J. Feldman, N. B. Gilula, and J. D. Pitts, editors. Chapman and Hall, London. 37–60.
54. Stewart, W. W. 1978. Functional connections between cells as revealed by dye-coupling with a highly fluorescent naphthalimide tracer. *Cell.* 14:741–759.
55. Unwin, N., and G. Zampighi. 1980. Structure of the junction between communicating cells. *Nature* (*Lond.*). 281:545–549.
56. Vial, J., and K. R. Porter. 1975. Scanning microscopy of dissociated tissue cells. *J. Cell Biol.* 67:345–360.
57. Weibel, E. R., Stäbli, W., Gnäghi, H. R., and Hess, F. A. 1969. Correlated morphometric and biochemical studies of the liver cell. *J. Cell Biol.* 42:68–91.
58. Wolpert, L. 1978. Gap junctions; channels for communication in development. *In* Intercellular Junctions and Synapses. J. Feldman, N. B. Gilula, and J. D. Pitts, editors. Chapman and Hall, London, 81–96.
59. Wondergem, R., and Harder, D. F. 1980. Membrane potential measurements during liver regeneration. *J. Cell Physiol.* 102:193–198.
60. Yancey, S. G., D. Easter, and J.-P. Revel. 1979. Cytological changes in gap junctions during liver regeneration. *J. Ultrastruct. Res.* 67:229–242.
61. Yee, A. 1973. Studies on the origin and distribution of intercellular junctions in regenerating liver. Ph.D. thesis, Harvard University. Cambridge, Massachusetts.
62. Yee, A., and J.-P. Revel. 1978. Loss and reappearance of gap junctions in regenerating liver. *J. Cell Biol.* 78:554–564.